

Evaluation of the Tropical Rainfall Measuring Mission (TRMM) 3B42 and 3B43 products relative to Synoptic Weather Station Observations over Cameroon

Roméo S Tanessong¹, P Moudi Igri², Roméo S Tanessong¹, Derbetini A Vondou³, Wilfried M Pokam³, J Taguemfo Kammalac³, S Kaïssassou³, G M Guenang³, A J Komkoua Mbienda³, and Yepdo Djomou³

¹University of Dschang

²Climate Prediction and Application Centre for Central Africa (CAPC-AC)

³University of Yaounde

November 24, 2022

Abstract

The Tropical Rainfall Measuring Mission (TRMM) daily (3B42) and monthly (3B43) rainfall products are evaluated relative to synoptic weather station observations in Cameroon and according to the main agro-climatic regions. In order to achieve this goal, deterministic and categorical metrics were used, as well as inter annual variability and seasonal distributions. Outcomes of the comparison showed that synoptic weather station data are strongly correlated with the TRMM 3B43 data and that rainfall distribution is characteristic for each agro-climatic region. The highest skill scores were observed in the Sudano-sahelian, High Savannah, and Western Highlands zones, while the Uni-modal Equatorial zone displayed the lowest correspondence scores between TRMM rainfall estimates and station-based observations. Daily TRMM 3B42 showed good performance in detecting rainy events, especially for light and moderate intensity rainfall events. TRMM 3B42 overestimates rainfall intensities except in the uni-modal region where rainfall intensities are underestimated. Rainfall seasonality, as well convective zone are well reproduced by the TRMM datasets. Overall, the skill of TRMM 3B42 decreases for increasing precipitation intensities.

Evaluation of the Tropical Rainfall Measuring Mission (TRMM) 3B42 and 3B43 products relative to Synoptic Weather Station Observations over Cameroon

P. Moudi Igri ^{a,c,d}, Roméo S. Tanessong ^{b,d,*},

Derbetini A. Vondou ^d, Wilfried M. Pokam ^{e,d},

J. Taguemfo Kammalac ^d, S. Kaissassou ^{h,d}, G. M. Guenang ^{f,d},

A. J. Komkoua Mbienda ^{f,d}, Zéphirin Yepdo Djomou ^{g,d},

^a*Climate Prediction and Application Centre for Central Africa (CAPC-AC),
Department of Weather and Climate Research and Application (DWCRA)*

^b*School of Wood, Water and Natural Resources, Faculty of Agronomy and
Agricultural Sciences, University of Dschang, Cameroon, PO Box 786, Ebolowa*

^c*Agence pour la Sécurité de la Navigation Aérienne en Afrique et à Madagascar
(ASECNA)*

^d*Laboratory for Environmental Modeling and Atmospheric Physics (LEMAP),
University of Yaounde 1, Cameroon. PO.Box: 812 Yaounde, Cameroon*

^e*Department of Physics, High Teacher Training College, University of Yaounde 1,
P.O. Box 47, Yaounde, Cameroon*

^f*Laboratory of Mechanics and Modeling of Physical Systems, Department of
Physics, Faculty of Science, University of Dschang, Po Box 67, Dschang,
Cameroon*

^g*Climate Change Research Laboratory, National Institute of Cartography, P.O. Box
157 Yaounde, Cameroon*

^h*Department of Electrical and Telecommunication Engineering, National Advanced
School of Engineering, University of Yaounde 1 P.O. Box 8390, Yaoundé,
Cameroon*

1 Abstract

2 The Tropical Rainfall Measuring Mission (TRMM) daily (3B42) and monthly
3 (3B43) rainfall products are evaluated relative to synoptic weather station obser-
4 vations in Cameroon and according to the main agro-climatic regions. In order to
5 achieve this goal, deterministic and categorical metrics were used, as well as inter-
6 annual variability and seasonal distributions. Outcomes of the comparison showed
7 that synoptic weather station data are strongly correlated with the TRMM 3B43
8 data and that rainfall distribution is characteristic for each agro-climatic region.
9 The highest skill scores were observed in the Sudano-sahelian, High Savannah, and
10 Western Highlands zones, while the Uni-modal Equatorial zone displayed the lowest
11 correspondence scores between TRMM rainfall estimates and station-based obser-
12 vations. Daily TRMM 3B42 showed good performance in detecting rainy events,
13 especially for light and moderate intensity rainfall events. TRMM 3B42 overesti-
14 mates rainfall intensities except in the uni-modal region where rainfall intensities are
15 underestimated. Rainfall seasonality, as well convective zone are well reproduced
16 by the TRMM datasets. Overall, the skill of TRMM 3B42 decreases for increasing
17 precipitation intensities.

18 *Key words:* TRMM 3B42, TRMM 3B43, rain gauge, synoptic weather station,
19 satellite based rainfall

20 1 Introduction

21 Climatic excess and deficit rainfall associated with floods and droughts respectively, greatly
22 impact socio-economic activities such as agriculture and water resource management, as
23 well as on human livelihoods, particularly in developing countries with agriculture-based
24 economies and vulnerable populations. Therefore, rainfall plays many important roles in

* Corresponding author

Email address: tanessrs@yahoo.fr (Roméo S. Tanessong).

25 the Earth system, including being the primary source of freshwater, defining conditions
26 for diverse ecosystems, and enabling economic activities. As such, rainfall information from
27 any given hydrological system is of crucial importance (Munzimi et al 2015), characterizing
28 Congo Basin rainfall and climate using Tropical Rainfall Measuring Mission (TRMM) satel-
29 lite data and limited rain gauge ground observations. With shifting seasons, increasing water
30 scarcity, and potentially more frequent and intense extreme events (Change 2007; Field et al
31 2012), climate change is bringing a series of disasters and livelihood impacts to the poorest
32 and most vulnerable countries and communities, and is placing development assistance at
33 risk. Over the past decades, progressively more attention has been given to converging Dis-
34 aster Risk Reduction (DRR) and Climate Change Adaptation (CCA) agendas conceptually
35 and in practice at sub-national, national, and international levels (Tom et al 2010). A good
36 knowledge of climatic information is crucial to achieve such programs, particularly weather
37 forecasts and climate change model-based projections. Such information are necessary for
38 policy makers for efficient planning at national and regional scale.

39 The West and Central Africa regions have been identified by the United Nations as one
40 of the nine "hot spots" of the world for environmental changes (Koster et al 2004). These
41 regions have also experienced the largest decrease in rainfall over the past 60 years, despite a
42 partial return to normal since 1990 (Aich et al 2013; Roudier et al 2014; Vrieling et al 2013;
43 Yepdo et al 2009; Mohino et al 2010). In Central Africa particularly, numerous studies (e.g.
44 Raghavendra et al 2020; Zhou et al 2014; Hua et al 2016, 2018; Jiang et al 2019) pointed
45 out the long-term drying and rainfall decline in this region. For example, Raghavendra et al
46 (2020) found a significant increase in the number of dry Madden-Julian Oscillation (MJO)
47 days (3.47 days/decade) tending to intensify the large-scale drying trend over the Congo dur-
48 ing October–March which enhances the net drying trend by 13.6% over the Congo. Zhou et al
49 (2014) presented observational evidence for a widespread decline in forest greenness over the
50 past decade based on analyses of satellite data and argued that the decline in vegetation
51 greenness, particularly in the northern Congolese forest is generally consistent with decreases
52 in rainfall, terrestrial water storage and water content. Similarly, Jiang et al (2019) showed

53 that the dry season length in the Congo basin increased by 6.4–10.4 days per decade in the
54 period 1988–2013 attributed to an earlier dry season onset caused by long-term droughts due
55 to decreased rainfall in the pre-dry season (April–June).

56 Until the 1970s, studies have focused on the annual cycle of rainfall and variability with-
57 out really understanding its inter-annual variability (Pohl 2007; Samba and Nganga 2012;
58 Nicholson et al 2019; Vondou et al 2010a, 2010b; Sandjon et al 2012, 2014; Zebaze et al 2017;
59 Kamsu-Tamo et al 2014). These studies have clearly demonstrated the importance of the
60 equatorial Walker-type circulation over the Congo basin. Hua et al (2016) investigated the
61 possible causes of the Central Equatorial African long-term drought and found that the
62 drought results primarily from Sea Surface Temperature (SST) variations over Indo-Pacific
63 associated with the enhanced and westward extended tropical Walker circulation associated
64 with reduced low-level moisture transport and weaker West African monsoon. What does
65 clearly emerge from the various studies is that factors in rainfall variability vary tremendously
66 within equatorial Africa and that the regionalization of the factors and the factors themselves
67 vary by season (Nicholson et al 2019). Climate and environmental monitoring in this region,
68 by taking into account the various factors and to potentially predict future changes, require
69 detailed knowledge of the rainfall distribution at different timescales. This was once available,
70 as thousands of stations were operative in equatorial Africa in the mid-twentieth century.
71 However, in most countries of equatorial Africa, the networks have continually declined since
72 the 1970s or 1980s (Nicholson 2018; Nicholson et al 2019; Guenang and Mkankam-Kamga
73 2012; Sultan and Janicot 2004; Washington et al 2013). Munzimi et al (2015) stated that
74 with station data being sparse, not covering concurrent time periods, and having incom-
75 plete time series, achieving consistency is a challenge, while Dinku et al (2007) reported that
76 the number of rain gauges throughout Africa is small and unevenly distributed, and the
77 gauge network is deteriorating. Satellite rainfall estimates are being used widely in place of
78 gauge observations or to supplement gauge observations. Thus, climate model outputs and
79 water resource management, particularly in regions with sparse ground based observations
80 are inherently prone to uncertainties. In such cases, validations with reanalysis data have

81 shown promise, particularly when knowledge of the state of the atmosphere on a uniform
82 grid is required (Mooney et al 2011). In addition to re-analysis datasets, useful rainfall es-
83 timates have been derived from space missions devoted to measuring precipitation such as
84 the Tropical Rainfall Mission Measurement (TRMM) (Huffman et al 2001; Huffman et al
85 2007). Numerous studies compared these datasets with in situ observations (Roads et al
86 1992; Pocard et al 2000; Nicholson et al 2003, 2019; Camberlin et al 2019; Munzimi et al
87 2015) and evaluated Regional Climate Models (RCM)(Lowrey and Yang 2008; Flaounas et al
88 2010; Tchotchou and Mkankam-Kamga 2010; Igri et al 2015, 2018; Tanessong et al 2014,
89 2017; Komkoua Mbienda et al 2017a, 2017b; Tamoffo et al 2019a, 2019b; Fotso-Nguemo et al
90 2017a, 2017b), including temperature (using ERA-Interim reanalysis data) and precipita-
91 tion (using TRMM data). They found that satellite rainfall products can be used as refer-
92 ence data for model validation without having a good knowledge on their associated errors.
93 Pocard et al (2000) compared rainfall structures in the National Centers for Environmental
94 Prediction (NCEP)/National Center for Atmospheric Research (NCAR) dataset and in situ
95 observations across tropical Africa, showing that the reanalysis rainfall is closer to the ob-
96 servation in regions with a single rainy season per year. More recently, Munzimi et al (2015)
97 tested and reported the use of limited rainfall gauge data within the Democratic Repub-
98 lic of Congo (DRC) to recalibrate a TRMM science product (TRMM 3B42, version 6) in
99 characterizing precipitation and climate in the Congo basin. They compared and adjusted
100 Rainfall estimates from TRMM using ground precipitation data from 12 DRC meteorological
101 stations from 1998 to 2007. They found that version-6 TRMM 3B42 data are appropriate for
102 quantifying Congo basin rainfall regimes and for deriving climate maps when calibrated by
103 ground gauge datasets from within the region and that the version-7 TRMM 3B43 product
104 accurately depicted Congo basin precipitation without bias. Nicholson et al (2019) evaluated
105 a set of satellite rainfall products and the Global Precipitation Centre Climatology (GPCC)
106 gauge dataset over the Congo basin for the 1983–94, and 1998–2010 periods. They found a
107 good linkage between several products in respect with in situ data. Furthermore, they stated
108 that the performance of the products evaluated is notably poorer in recent years (1998–
109 2010), when the station network is sparse, than during the period 1983–94, when the dense

110 station network provides reliable estimates of rainfall. In their study, Camberlin et al (2019)
111 made an intercomparison of seven gridded rainfall products incorporating satellite data over
112 Central Africa. They reported that there is an overall good reproduction of the mean rainfall
113 regimes and the spatial patterns of mean annual rainfall, though some discrepancies exist in
114 the longitudinal distribution of rainfall along the Equator from Gabon to the eastern DRC.

115 While, in principle, satellite data now provide the needed spatial detail, the available satellite
116 products have generally been validated only over eastern equatorial Africa, a region very dif-
117 ferent climatically from the Congo basin. Two validations that did emphasize the Congo basin
118 found large discrepancies between gauge and satellite data (McCollum et al 2000; Yin et al
119 2004). Negrón Juárez et al (2009) and Sun et al (2018) similarly found satellite estimates of
120 rainfall to be poor over equatorial Africa, with wide discrepancies among the various satellite
121 products. This was particularly the case for the Congo basin.

122 Despite the availability of these recent works to understand climate change and variability
123 over the Congo rainforests, the physical mechanisms involved are only partially understood
124 (e.g., Hua et al 2018; Jiang et al 2019). This knowledge gap is further aggravated over Africa
125 (especially the Congo) due to the relative lack of fundamental research and absence of field
126 measurements (e.g., Washington et al 2013; Lee and Biasutti 2014; Alsdorf et al 2016) when
127 compared to other parts of the world including the Congo's counterpart the Amazon rainfor-
128 est (Alsdorf et al 2016). In addition, the case of Cameroon is more specific and challenging
129 due to the fact that the country has five different climate regimes (hereafter called ecologi-
130 cal zones). Unfortunetely, limited studies investigated the Cameroon's complexity climate
131 which belong separetely to the Congo basin and to the saharan-sahelian climate regimes,
132 with a huge sensitivity to orography, coastal circulation and easterly waves. This study aims
133 at evaluating the performance of TRMM datasets over Cameroon through a comparison
134 with synoptic weather station observations. We will investigate the inter-annual, seasonal
135 and daily distributions, evaluate the dynamics associated to rainfall types and heavy rainfall
136 occurrences. The time period for the evaluation covers the overlap between in situ obser-
137 vations and TRMM data, i.e. 1998-2008 and 1998-2000, respectively. The outcomes of the

138 study will provide insights into how synoptic weather station data and satellite-based rain-
139 fall estimates can be used optimally to characterise rainfall patterns over Cameroon's main
140 ecological zones.

141 The present study is organized as follows : Section 2 presents the study area with agro-
142 climatic zones in Cameroon. Section 3 describes the data. Section 4 provides the methodology
143 used. Section 5 describes the major results obtained from the study and Section 6 is devoted
144 to the discussion.

145 **2 Study area: Agro-climatic zones in Cameroon**

146 The study region in Cameroon (2°N-14°N and 9°E-16°E) encompasses five distinct agro-
147 ecological zones as shown in Fig. 1 (Bele et al 2013).

148 The Sudano-sahelian zone encompasses the northernmost regions of the country and is char-
149 acterised by mean annual rainfall of 800 mm/year. This zone is the driest with the high-
150 est temperatures and the most sunshine hours. The Guinea Savannah zone includes the
151 Adamaoua region (mean annual rainfall approximately 1500 mm/year), characterised by
152 high elevation and cool temperatures throughout the year. The Bi-modal Equatorial zone
153 is the largest (average rainfall approximately 2000 mm/year, mean annual temperature ap-
154 proximately 25°C) and is characterised by two distinct dry seasons: a short dry season and a
155 long dry season. The Mono-modal Equatorial zone, situated along the coast, is the rainiest
156 with 2500 mm/year annual rainfall due to humidity from the Atlantic Ocean and sea breeze
157 modulating temperatures. The Western Highlands zone is characterised by climatic features
158 similar to the Guinea Savannah zone.

160 *3.1 In situ Rainfall Observations: National Meteorological and Hydrological Services (NMHS)*
161 *data*

162 Hourly rain gauge rainfall records (mm/hour) from 21 stations across Cameroon were ob-
163 tained from NMHS as shown in Fig. 2 and coverage of the dataset is summarised in Table
164 1. Homogeneity tests were carried out to analyse the homogeneity of the stations data. The
165 results of these tests (not shown here) show that several stations are homogeneous.

166 *3.2 Satellite Based Rainfall Estimates: TRMM datasets*

167 The Tropical Rainfall Measuring Mission (TRMM), a joint mission of the US National
168 Aeronautics and Space Administration (NASA) and the Japanese National Space Devel-
169 opment Agency (NASDA), provided data on precipitation in the tropics and subtropics
170 (Huffman et al 2007). TRMM 3B42 V7 (daily rainfall estimates) and TRMM 3B43 V6 (mean
171 monthly rainfall estimates), both on a $0.25^\circ \times 0.25^\circ$ grid were obtained from the NASA web
172 site (<http://trmm.gsfc.nasa.gov/>) for the evaluation undertaken here.

173 *3.3 Climate Hazards InfraRed Precipitation with Stations (CHIRPS)*

174 The CHIRPS dataset (Funk et al, 2015) were developed by the U.S. Geological Survey
175 (USGS) and the Climate Hazards Group at the University of California. Quasi-global gridded
176 products are available from 1981 to near-present at 0.05° spatial resolution (5.3 km) and at
177 pentadal, dekadal, and monthly temporal resolution. CHIRPS data were used in this study to
178 represent the spatial distribution of the climatology (1983-2013) of the annual accumulated
179 rainfall.

180 4 Methodology for TRMM Evaluation

181 The evaluation of TRMM rainfall products relative to in situ observations at rain gauges is
182 carried out according to the weather station in the five agro-ecological zones in Cameroon
183 because rainfall distribution is correlated with vegetation productivity and thus will allow
184 water resources management according to each region. TRMM data at $0.25^\circ \times 0.25^\circ$ grid
185 scales containing rain gauges are compared with the in situ observations at the daily and
186 monthly time steps. TRMM grids selected in this study are those in which the stations
187 are located. Commonly used deterministic metrics such as mean error (ME), correlation
188 coefficient (CC), mean absolute error (MAE), and root mean square error (RMSE) were
189 used to quantify differences between TRMM and gauge data (Igri et al 2015). ME is simply
190 the difference between the average satellite-based estimates and average observed rainfall,
191 and therefore expresses the bias of the satellite-based estimates rainfall. The CC (perfect
192 value 1) indicates the degree of correspondence between the satellite-based estimates and
193 observed rainfall. MAE (perfect value 0) is the arithmetic average of the absolute values of
194 the differences between the TRMM and observations. Similarly, the RMSE (perfect value 0)
195 measures the error magnitude, but gives more weight to the larger errors.

196 Additionally, categorical statistics were computed (Wilks et al 2006) on the basis of 2×2
197 contingency table of rainfall occurrence (Table 2) where h is the number of hits (rainfall
198 correctly detected in TRMM and observed at the gauge), f is the number of false alarms
199 (rainfall detected in TRMM, but not observed at the gauge), m is the number of misses
200 (rainfall observed at the gauge, but not detected in TRMM), and c is the number of correct
201 negatives (no rainfall observed at the gauge and no rainfall detected in TRMM), with $N =$
202 $h + f + m + c$, representing the total number of gauge-grid cell pairs (Ebert et al 2007) .

203 Categorical statistics ratio bias (BIAS), probability of detection (POD), probability of false
204 detection (POFD), and the equitable threat score (ETS) are computed as follow:

$$205 \quad BIAS = \frac{h + f}{h + m}, \quad POD = \frac{h}{h + m}, \quad POFD = \frac{f}{f + c}, \quad ETS = \frac{h - k}{h + f + m - k} \quad (1)$$

206 where k is given by

$$207 \quad k = \frac{(h + m)(h + f)}{h + f + m + c} \quad (2)$$

208 The ratio bias (BIAS) is the ratio of satellite-based rainfall estimates to observed rainfall
209 events; a BIAS score above 1.0 indicates overestimation of the number of rain events in
210 satellite data, and a score below 1.0 underestimation (Scheel et al 2011; Cai et al 2016).
211 POD evaluates the ability of TRMM 3B42 to detect rainfall events. POFD is the percentage
212 of the observed no rain events, which were incorrectly estimated as rain events in the satellite
213 data. ETS evaluates how skilful satellite-based rainfall estimates are relative to rain gauge
214 observations, and the scores can be compared equally across different regimes.

215 The statistical measures above are calculated for the daily, monthly, and annual time series
216 of TRMM-gauge pair time series data, and the results are presented and discussed according
217 to agro-ecological zones.

218 **5 Results**

219 *5.1 Monthly to annual timescale rainfall variability*

220 Fig. 3 shows the mean monthly accumulated rainfall according the to five agro-ecological
221 zones. As displayed in Fig.3, the Sudano-Sahelian is the driest zone in Cameroon. It re-
222 ceives approximately on average 3 months of rainfall during the African monsoonal period
223 (Vondou et al 2010b; Tchotchou and Mkankam-Kamga 2010). The rainy season effectively
224 starts in June and ends in September. Maximun rainfall occurs in august with over 200 mm
225 in Garoua and Kaele. Rainfall occurrences are generally highly convective. The remaining
226 period, ie from october to may is the dry period. This zone, which encompasses the Maroua,
227 Garoua main cities, is the most vulnerable zone of the country to extreme events such as
228 droughts and floods. In addition, population living in this area are the most exposed to
229 famine (Guenang and Mkankam-Kamga, 2012; Penlap et al, 2004).

230 For the Highs Savannahs zone of Cameroon also called the Adamawa region, both TRMM
231 algorithm and Ground Data (GD) in these stations (Ngaoundere, Banyo and Touboro) have
232 similar seasonal distributions during the monsoon period, especially in august when rainfall
233 occurrence reaches its peak. Discrepancy between these datasets is particularly more high-
234 lighted in Banyo where TRMM retrieved data overestimate the GD. The correspondence
235 between the two datasets is more readily compared by displaying statistic scores.

236 Furthermore, in the Highlands zone (Bamenda, Dschang and Kundja), the global tendency is
237 overestimation by GD. Maximum rainfall occurs in august and the dry season is identified to
238 be in December-January-February (DJF). Ones more in this zone, there is a good agreement
239 between TRMM algorithms and GD.

240 The difference between TRMM 3B43 data and GD is remarkable in the forest zones. The
241 main feature is overestimation by 3B43. Monthly mean zonal analysis for the study period
242 in this zone reveals that such features are persistent during the whole year. This tendency is
243 generally less in DJF and is strongest in June-July-August-September (JJAS) when rainfall
244 is highest as this period corresponds to the monsoon period. But, an exception behavior has
245 been shown in the Douala station where TRMM data are underestimated all over the study
246 period.

247 In addition, mean monthly comparisons between rain gauge precipitation and TRMM 3B43
248 for the different zones averaged from 1998 to 2008 revealed that, in general, GD showed
249 closer agreement with 3B43 algorithms, although GD in stations in the Northernmost parts
250 of Cameroon (Kaele, Garoua, Ngaoundere, Banyo, Touboro) have the closest agreement with
251 3B43 data compared to the Southernmost parts ones, specially in the uni-modal (Newsonne,
252 Mukunje, Mpundu, Nkongsamba) and bi-modal Equatorial zones(Abong-Mbang, Akono-
253 linga, Bertoua, Ambam, Bertoua, Ebolowa).

254 Fig.4 and Fig.5 represent the annual correlation and the annual bias of rainfall distribution
255 respectively in the different stations.

256 As stated earlier, the global tendency is overestimation by TRMM algorithm. Both datasets
257 statistically agree by displaying high annual correlation. For example, annual correlation in
258 Ngaoundere station (Fig.4) is at least 0.85 during the eight years of available data (from
259 1998 to 2005). In Fig.5, the mean annual biases are plotted over the available data for the
260 five zones. The biases appear to be random with either overestimation or underestimation
261 and ranging from -18 mm to 14 mm. This analysis tends to confirm the trend seen in Fig.3.
262 Moreover, the annual correlation (Fig.4) is generally higher than 70% in the whole study
263 period. It can be partially concluded that TRMM has a good performance over the soudano-
264 sahelian zone. Comparison made with other zones exhibits in general cases that the rainfall
265 peak in this agroecological zone is the lowest one all over the four zones.

266 Comparatively, TRMM data more agree with the GD in sahelian zone. Fig.4 shows a good
267 correlation coefficient between GD and TRMM datasets which reaches 0.8 on average in
268 this zone. During the studied years, statistic parameters are significant at the level of 95% of
269 confidence using t-test. In general, negative biases are found in Kaele and Garoua, that lead to
270 a strong tendency to overestimation by GD, although there is a remarkably good agreement
271 between the TRMM and GD in March-April-May (MAM) and August-September-October-
272 November (ASON). All over this period, in the sahelian zone, TRMM shows the rainfall
273 peak (240 mm/month) in Kaele and Garoua in August which is roughly like those provide
274 by the GD and this month is therefore the rainiest one.

275 Moreover, the underestimation at Douala station is blamed to a large-fraction of warm rain
276 (hard to detect from algorithms based on cold IR temperatures and 85 GHZ ice scattering)
277 and changes in the TRMM rainfall estimations over land and sea (over ocean, the 37 GHZ
278 channel allows for direct rainfall estimates). Such changes create "boundary effects" at the
279 coast. Exception behavior shown in the Douala station in the annual distribution can also
280 be partially attributed to sea-breeze (Vondou et al 2010b).

281 In the above mentioned zones, 3B43 closely matches the rain GD, except in the Bi-modal
282 Equatorial zone (Fig.7) where 3B43 has the worst agreement. The highest negative biases are

283 recorded in the Douala station with values reaching -110 mm/year and the highest positive
284 biases are recorded in the Mpundu station with the values higher than 200 mm/year (see
285 Fig.5). In general, the best agreements are obtained in the Sahel, Savannah and Highlands
286 zones. Also, in comparison with other regions, forest zone has the poorest agreement for
287 all the years considered. This can be caused by orographic effects or other synoptic pertur-
288 bations. In uni-modal Equatorial zone, the poorest agreements with rain GD are recorded
289 during the monsoon period, corresponding to the peak of the wet season June-July-August
290 (JJA). This zone has the worst correlation, while for the Sahel, Savannah and Highlands
291 regions the correlations are generally higher than those obtained in the forest zones. Overall,
292 monthly to annual rainfall distribution in Cameroon is strongly linked to the tropical rain
293 belt position as shown in Fig.6.

294 When the tropical rain belt reaches its maximum position (around 20°) in August-September,
295 the driest region of the country (the soudano-sahel zone) receives its maximum precipitation.
296 This feature is also noticed for the others zones of the country, especially for uni-modal distri-
297 bution regions. Thus, uni-modal rainfall distribution is typically modulated by the seasonal
298 tropical rain belt variability. Retreat and onset of the rainfall can also be explained by the
299 tropical rain belt southernmost (minimum value) and northernmost (maximum value) posi-
300 tions as displayed in Fig.6. For instance, when the tropical rain belt reaches its southernmost
301 position, especially between november and march, the whole country is in the dry season
302 characterized meteorological phenomena such as haze and sand with visibility less than 4000
303 meter in average. This feature matches the TRMM data as shown in Fig.3.

304 *5.2 Daily station rainfall*

305 Daily time series of accumulated rainfall are presented for six (6) stations for the years 1998,
306 1999 and 2000 in Fig.7 and Fig.8.

307 Difference between daily in situ observation and TRMM precipitation over these regions
308 can be clearly seen in the amplitude of the peak. 3B42 overestimates in situ observations

309 by showing higher precipitation amount in all the stations for the whole period. In addi-
310 tion, overestimation is more pronounced during monsoon period when stations receive their
311 maximum rainfall amount. In the meantime, daily rainfall reproduces the same features as
312 depicted by monthly and annual time scales rainfall series for different regions. Year to year
313 rainfall variability follow the same daily time series over all stations. The overestimation that
314 occurs in 3B42 is largely attributed to the cold top clouds, to the retrieval algorithm that
315 fail to consider the altitude of an object (Scheel et al 2011) .

316 Fig.9 shows the categorical indices for mean daily rainfall and linear regression fitting for
317 years 1998 to 2000 for Bertoua, Garoua, Maroua, Douala, Ebolowa, Ngaoundere and Yaounde
318 stations.

319 The figure has been shown in order to estimate the accuracy of 3B42 and to assess its
320 performance in detecting precipitations amount. Numerical difference in rain amounts shows
321 overestimation of daily rainfall as shown by a negative ME over different stations. The
322 average error magnitude measured by RMSE and MAE depicts significant difference between
323 3B42 and rain gauges data. Whereas, correlations are moderate (0.5) between 3B42 and
324 rain gauges data for all stations. The correspondence indicates the performance of 3B42 in
325 estimating precipitations in certain extent (Cai et al 2016).

326 In Fig.10, we display the sensitivity of categorical indices (BIAS, POD, POFD and ETS) to
327 the rainfall thresholds extending from 0.1 mm/day to 35 mm/day that we consider as light
328 to heavy rainfall.

329 In terms of occurrences, rainy events are overforecasted by 3B42 with a BIAS (frequency
330 bias) greater than 1 (Fig.10(a)), except for Douala station where rain events are underfore-
331 casted for rainfall threshold less than 2 mm/day. In general, the global trend is increasing
332 in BIAS score with rainfall threshold. A sudden shift and rapid increasing is observed in
333 BIAS trend for rainfall thresholds greater than 10 mm/day, suggesting that 3B42 capability
334 worsens in detecting heavy rainfall. The tendency is similar for all the stations, no matter the
335 agroecological zones. The strange behavior in Douala station could be attributed to bound-

336 ary effects as mentioned above leading to cold bias. For the three remaining indices (Fig.10
337 (a), (b) and (c)), the global trend is a significant decreasing with an increasing threshold.

338 The POD is very significant (more than 60%) for light rainfall. When daily precipitation
339 intensity increases from moderate to heavy, only less than 40% of rainfall is detected by
340 3B42. A close look at the POD distribution shows that 3B42 in Ngaoundere and Bertoua
341 stations performs well in detecting heavy rainfall, with at least half of rain events detected. In
342 general, POD indicates that 3B42 can only correctly estimate light to moderate rain events
343 with sufficient credibility. This finding is similar to the results found by Cai et al (2016).
344 However, POFD consistently decreases with daily precipitation intensity as shown by Fig.10
345 (d). Special tendency is shown by Maroua and Garoua stations, where we have a better
346 score of POFD. No rain events incorrectly forecasted in these stations are the best even
347 for heavy rainfall. This trend is in accordance with the good performance of 3B43 in these
348 regions as shown in the previous sections. Moreover, satellites estimates in these regions are
349 generally the best because they only receive rainfall during the monsoon period with is more
350 calibrated by satellites sensors and where no boundary effects are present (no forests and no
351 sea vicinity).

352 As POFD can characterize the fraction of the case that the observed no rain day is mistakenly
353 identified as rain day by 3B42, so it is evident that 3B42 is more likely to regard no rain
354 day as rain day incorrectly for light rain intensity. Though it shows a poorer score of POFD
355 for light rain intensity than that for heavy rain intensity, much better scores of POD, BIAS,
356 even the comprehensive index ETS are obtained for light rain intensity. Thus, 3B42 has a
357 higher probability to correctly identify numerous light rain events with an improved accuracy
358 compared to heavy rain event, as stated by Cai et al (2016). In general all stations located
359 in forest zones (uni modal and bi modal) and in the Highland zones show scores that are
360 lower, likely due to the mountainous terrain and related high spatial rainfall variability
361 where stations show low spatial representativeness, introducing large uncertainties as found
362 by (Monsieurs et al 2018; Camberlin et al 2019).

363 6 Discussion

364 Figure 11 displays the interannual Hovmöller diagrams of the monthly accumulated convec-
365 tive rainfall and climatology for the period 1998–2008. Two main convective precipitation
366 cores are found around 6°N–8°N centered on May and October and around 10°N–12°N cen-
367 tered on July. The core found in May is the most intensive when compared to others and
368 the one in July is less intense than the one in October. This dynamic is consistent with the
369 uni-modal and bi-modal rainfall distribution in the forest zones. The more important finding
370 is that although the convective core found in April–May is the most intensive, the rainy-
371 season peaks in this period is drier than the rainy-season peaks in October, highlighting a
372 seasonality variation with respect to the stations distance to the equator where rainfall peak
373 in the bi-modal region occurs during transitional seasons, corresponding to the northward
374 passage of the rain belt in April and southward passages of the rain belt in October as found
375 by Jiang et al (2019). When the tropical rain belt (TRB) is at its southernmost position, con-
376 vection occurs around the 6°N with the core during the transition months (April, May) and
377 October, consistent with the results obtained by Raghavendra et al (2018) and Munzimi et al
378 (2015) who found that the passage of the intertropical convergence zone (ITCZ) results in
379 two local rainy and dry seasons of varying length and intensity. The high intensity of thunder-
380 storm in April results in less cumulative rainfall compared to the October’s rainfall peak. This
381 feature could be caused by moisture being transported deeper into the upper troposphere
382 during April transition month (thunderstorms are more powerful in April than in Octo-
383 ber), resulting in lesser moisture available to rain down to the surface (Raghavendra et al,
384 2018), an increase in virga (Sassen and Krueger, 1993) and high recycling ratio of water over
385 the Congo Basin (e.g., Pokam et al 2012; Dyer et al 2017). Raghavendra et al (2018) also
386 reviewed that the width (wide or narrow) and the strength (intensity, number and area) of
387 the TRB coupled with the expanding of the Hadley cell (Byrne and Schneider, 2016) can
388 partly explain the occurrence of stronger updrafts and higher heights of convective cloud.
389 Our results are also consistent with the results found by Camberlin et al (2019) where April
390 and October are found to be the rainfall peak months for both hemispheres. In the bi-modal

391 zone, the two rainy-season peaks are not “mirrored” or proportional (Munzimi et al, 2015).
392 The october peak found is wetter than the april because the origin of the water vapor fluxes
393 feeding the TRB varied by season. Suzuki (2011) stated that in April, the water vapor flux is
394 mostly derived from the Indian Ocean via Tanzania in the congo Basin, whereas in October,
395 the water vapor flux is supplied from within the Congo basin to whom belongs the bi-modal
396 zone of Cameroon and some stations west of the congo basin boundaries.

397 Figures 12 and 13 show the spatiotemporal distribution of the 90th percentile of the monthly
398 accumulated convective rainfall climatology (3A12) and the monthly accumulated non-convective
399 rainfall climatology (difference between 3B42 and 3A12). It comes out that most contribution
400 comes from convective precipitation for all months, except July, August and some extend
401 September where the most contribution comes from stratiform precipitation, especially in
402 the uni-modal and the Highland zone due to the vicinity of the coast (monsoon period). Even
403 if a significant portion of tropical rainfall is stratiform, however, Schumacher and Houze Jr
404 (2003) cited Central Africa as one of the areas where convective rain amounts are high and
405 stratiform rain fractions are low (20%–30%). We also found most convective areas localized
406 in the Highland and in the south of the Highs savannahs zones from March to May and in
407 October. During the monsoon period, convective precipitations are shifted north up to the
408 Sudano-Sahelian zone and are attributed to the onset of the West African monsoon, which
409 dominates the circulation between May–August (Sultan and Janicot, 2003). The uni-modal
410 and bi-modal zones are strongly linked to the moonsson strength, whereas the soudano-
411 sahelian zone is most linked to Mesoscale Convective System (MCS) associated to African
412 easterly waves activities (Nicholson et al 2003, 2019).

413 Furthermore, difference between total and convective precipitation (Figures 12 and 13) also
414 shows a non negligible contribution of stratiform rainfall in the Soudano-Sahelian (SS) zone.
415 In fact, some cities in Cameroon have experienced flooding events, mostly in the Far north
416 and the Littoral regions of Cameroon (located in the SS zone and the uni-modal-zone respec-
417 tively) during the monsoon period (Igri et al 2015, Tanessong et al 2017). We can therefore
418 conclude that heaviest rainfall are not always derived from tallest storms (in april and octo-

ber), as found by Hamada et al (2015). Although there is a strong correlation between convective and total precipitation, we can raise the fact that associated errors are still significant as shown in Figure 14. The Soudano-Sahelian zone shows lesser error than the others zones, while the uni-modal zone shows the highest error. The good correlation between convective precipitation and total precipitation in SS zone explains why most rainfall in this region is of convective origin. This convective activity is consistent with the south and north tropical rain belt (TRB) displacement. Using 3A12, we compared the distribution of 3B42 and 3B43 in order to highlight the contribution of convective precipitation in Cameroon. Precipitation distribution is modulated by the tropical rainbelt and the Madden-Julian Oscillation (MJO), not at the same frequency in the whole country, but with different intensity according to each ecological zone. With relation to MJO, Raghavendra et al (2020) found a significant distinction between rainfall amounts observed during the wet and dry RMM phases across different months of the year, while the migration of the tropical rainbelt strongly dictates seasonal rainfall amounts and thunderstorm activity (Nicholson 2018; Taylor et al 2018). Rainfall is typically enhanced during the wet Real-time Multivariate MJO Index (RMM) phase (phase 2) and reduced during the dry RMM phases (phases 5 and 6). The dry annual bias shown by TRMM, especially over the uni-modal zone could be explained by omitted rainfall events, specifically a lack of sensitivity to different types of rain by TRMM sensors. TRMM 3B42 data are also insensitive to light-rain events; such light-rain events, which are characteristic of stratiform rain in the region, are more frequent during the Congo basin dry season (Munzimi et al, 2015).

7 Conclusion

The objective of this study was to assess the correspondence between TRMM (3B42 et 3B43) and 21 weather stations unevenly distributed over Cameroon and representing different agro-climatic regions in terms of annual cycles, number and intensities of wet events, trying to point out those regions where the agreement is the best/the worst. In order to achieve this

445 goal, deterministic and categorical metrics were used. Annual rainfall cycles showed that
446 TRMM 3B43 slightly underestimates rainfall in the Sahel, Savannah and Highlands zones
447 whereas it overestimates in the uni-modal and bi-modal Equatorial zones. The discrepancies
448 are generally most pronounced in the bi-modal Equatorial zone. In general, the study showed
449 that 3B43 closely matches rain gauge data, suggesting that the goal of the TRMM algorithm
450 was largely achieved as stated by Debo and Kenji (2003). Therefore TRMM 3B43 can be
451 used as reference data for validating numerical weather forecast models as a replacement
452 of gauge data. For instance, the best agreements with rain gauge data are obtained in the
453 Cameroon northern zone (Soudano-saharian and High Savannah) rather than for its south-
454 ern counterpart leading to two majors climatic regions in Cameroon: the North region of
455 Cameroon with the rainy season in JJA and the South region with the rainy season ranging
456 from March to November. Meanwhile, daily 3B42 depicts a good performance in detecting
457 rainy events with a reasonable extent, especially for light and moderate rainfall. TRMM
458 3B42 overestimates rain events except in Douala where rain events are underestimated and
459 its performance decreases with precipitations intensities.

460 **Acknowledgments**

461 Authors want to thank the TRMM algorithm team and the NMHS for providing data for free.
462 Special thanks to NCAR Command Language (NCL) tool for visualizations (NCL 2016) .
463 Tarnavsky's contribution to this study was funded as part of NERC's support of the National
464 Centre for Earth Observation (NCEO).

465 **References**

- 466 Aich V, Liersch S, Vetter T, Huang S, Tecklenburg J, Hoffmann P, Koch H, Fournet S,
467 Krysanova V, Müller E, et al (2013) Comparing impacts of climate change on streamflow
468 in four large African river basins. *Hydrology & Earth System Sciences Discussions* 10(11)
- 469 Alsdorf D, Beighley E, Laraque A, Lee H, Tshimanga R, O’Loughlin F, Mahé G, Dinga
470 B, Moukandi G, Spencer RG (2016) Opportunities for hydrologic research in the Congo
471 Basin. *Reviews of Geophysics* 54(2):378–409
- 472 Bele MY, Tiani AM, Somorin OA, Sonwa DJ (2013) Exploring vulnerability and adaptation
473 to climate change of communities in the forest zone of Cameroon. *Climatic Change* 119(3-
474 4):875–889
- 475 Byrne MP, Schneider T (2016) Narrowing of the ITCZ in a warming climate: Physical mech-
476 anisms. *Geophysical Research Letters* 43(21):11–350
- 477 Cai Y, Jin C, Wang A, Guan D, Wu J, Yuan F, Xu L (2016) Comprehensive precipita-
478 tion evaluation of TRMM 3B42 with dense rain gauge networks in a mid-latitude basin,
479 northeast, China. *Theoretical and applied climatology* 126(3-4):659–671
- 480 Camberlin P, Barraud G, Bigot S, Dewitte O, Makanzu Imwangana F, Maki Mateso JC,
481 Martiny N, Monsieurs E, Moron V, Pellarin T, et al (2019) Evaluation of remotely sensed
482 rainfall products over Central Africa. *Quarterly Journal of the Royal Meteorological Soci-
483 ety* 145(722):2115–2138
- 484 Change C (2007) IPCC fourth assessment report. *The Physical Science Basis* 2:580–595
- 485 Debo ZA, Kenji N (2003) Validation of TRMM radar rainfall data over major climatic regions
486 in Africa. *Journal of Applied Meteorology* 42(2):331–347
- 487 Dinku T, Ceccato P, Grover-Kopec E, Lemma M, Connor S, Ropelewski C (2007) Validation
488 of satellite rainfall products over East Africa’s complex topography. *International Journal
489 of Remote Sensing* 28(7):1503–1526
- 490 Dyer EL, Jones DB, Nusbaumer J, Li H, Collins O, Vettoretti G, Noone D (2017) Congo
491 Basin precipitation: Assessing seasonality, regional interactions, and sources of moisture.
492 *Journal of Geophysical Research: Atmospheres* 122(13):6882–6898

493 Ebert EE, Janowiak JE, Kidd C (2007) Comparison of near-real-time precipitation estimates
494 from satellite observations and numerical models. *Bulletin of the American Meteorological*
495 *Society* 88(1):47–64

496 Field CB, Barros V, Stocker TF, Dahe Q (2012) Managing the risks of extreme events and
497 disasters to advance climate change adaptation: special report of the intergovernmental
498 panel on climate change. Cambridge University Press

499 Flaounas E, Bastin S, Janicot S (2010) Regional climate modelling of the 2006 West African
500 Monsoon: sensitivity to convection and planetary boundary layer parameterisation using
501 WRF. *Clim Dyn* 363.:1083–1105

502 Fotso-Nguemo TC, Vondou DA, Pokam WM, Djomou ZY, Diallo I, Haensler A, Tchotchou
503 LAD, Kamsu-Tamo PH, Gaye AT, Tchawoua C (2017a) On the added value of the regional
504 climate model REMO in the assessment of climate change signal over Central Africa.
505 *Climate Dynamics* 49(11-12):3813–3838

506 Fotso-Nguemo TC, Vondou DA, Tchawoua C, Haensler A (2017b) Assessment of simulated
507 rainfall and temperature from the regional climate model REMO and future changes over
508 Central Africa. *Climate Dynamics* 48(11-12):3685–3705

509 Funk C, Peterson P, Landsfeld M, Pedreros D, Verdin J, Shukla S, Husak G, Rowland J,
510 Harrison L, Hoell A, et al (2015) The climate hazards infrared precipitation with stations—a
511 new environmental record for monitoring extremes. *Scientific data* 2:150,066

512 Guenang M G, Mkankam-Kamga F (2012) Onset, retreat and length of the rainy season over
513 Cameroon. *Atmos Sci Let* 13:120–127, DOI 10.1002/asl.371

514 Hamada A, Takayabu YN, Liu C, Zipser EJ (2015) Weak linkage between the heaviest rainfall
515 and tallest storms. *Nature communications* 6:6213

516 Hua W, Zhou L, Chen H, Nicholson SE, Raghavendra A, Jiang Y (2016) Possible causes
517 of the Central Equatorial African long-term drought. *Environmental Research Letters*
518 11(12):124,002

519 Hua W, Zhou L, Chen H, Nicholson SE, Jiang Y, Raghavendra A (2018) Understanding
520 the Central Equatorial African long-term drought using AMIP-type simulations. *Climate*
521 *dynamics* 50(3-4):1115–1128

522 Huffman G, Adler R, Morrissey M, Curtis S, Joyce R (2001) Global precipitation at one-
523 degree daily resolution from multi-satellite observations. *J Hydrometeor* 2:36–50

524 Huffman G, Adler R, Bolvin D, Gu G, Nelkin E, Bowman K, Hong Y, Stocker E, Wolff D
525 (2007) The TRMM Multi-satellite Precipitation Analysis (TPMA): Quasi-Global, Multi-
526 Year, Combined-Sensor Precipitation Estimates at Fine Scale. *J Hydrometeor* 8:38–55

527 Igri PM, Tanessong RS, Vondou D, Mkankam FK, Panda J (2015) Added-value of 3DVAR
528 data assimilation in the simulation of heavy rainfall events over West and Central Africa.
529 *Pure and Applied Geophysics* 172(10):2751–2776

530 Igri PM, Tanessong RS, Vondou D, Panda J, Garba A, Mkankam FK, Kamga A (2018) As-
531 sessing the performance of WRF model in predicting high-impact weather conditions over
532 Central and Western Africa: an ensemble-based approach. *Natural Hazards* 93(3):1565–
533 1587

534 Jiang Y, Zhou L, Tucker CJ, Raghavendra A, Hua W, Liu YY, Joiner J (2019) Widespread
535 increase of boreal summer dry season length over the Congo rainforest. *Nature Climate*
536 *Change* 9(8):617–622

537 Kamsu-Tamo P, Janicot S, Monkam D, Lenouo A (2014) Convection activity over the
538 Guinean coast and Central Africa during northern spring from synoptic to intra-seasonal
539 timescales. *Climate dynamics* 43(12):3377–3401

540 Komkoua Mbienda A, Tchawoua C, Vondou D, Choumbou P, Kenfack Sadem C, Dey S
541 (2017a) Impact of anthropogenic aerosols on climate variability over Central Africa by
542 using a regional climate model. *International Journal of Climatology* 37(1):249–267

543 Komkoua Mbienda A, Tchawoua C, Vondou D, Choumbou P, Kenfack Sadem C, Dey S
544 (2017b) Sensitivity experiments of RegCM4 simulations to different convective schemes
545 over Central Africa. *International Journal of Climatology* 37(1):328–342

546 Koster RD, Dirmeyer PA, Guo Z, Bonan G, Chan E, Cox P, Gordon C, Kanae S, Kowal-
547 czyk E, Lawrence D, et al (2004) Regions of strong coupling between soil moisture and
548 precipitation. *Science* 305(5687):1138–1140

549 Lee DE, Biasutti M (2014) Climatology and variability of precipitation in the twentieth-
550 century reanalysis. *Journal of climate* 27(15):5964–5981

551 Lowrey MRK, Yang ZL (2008) Assessing the capability of a regional-scale weather model
552 to simulate extreme precipitation patterns and flooding in central Texas. *Weather and*
553 *Forecasting* 23(6):1102–1126

554 McCollum JR, Gruber A, Ba MB (2000) Discrepancy between gauges and satellite estimates
555 of rainfall in equatorial Africa. *Journal of Applied Meteorology* 39(5):666–679

556 Mohino E, Janicot S, Bader J (2010) Sahel rainfall and decadal to multi-decadal sea surface
557 temperature variability. *Climate Dyn* doi:10.1007/s00382-010-0867-2.

558 Monsieurs E, Kirschbaum DB, Tan J, Maki Mateso JC, Jacobs L, Plisnier PD, Thiery W,
559 Umutoni A, Musoni D, Bibentyo TM, et al (2018) Evaluating TMPA rainfall over the
560 sparsely gauged East African Rift. *Journal of Hydrometeorology* 19(9):1507–1528

561 Mooney PA, Mulligan FJ, Fealy R (2011) Comparison of ERA-40, ERA-Interim and
562 NCEP/NCAR reanalysis data with observed surface air temperatures over Ireland. *Inter-*
563 *national Journal of Climatology* 31(4):545–557

564 Munzimi YA, Hansen MC, Adusei B, Senay GB (2015) Characterizing Congo basin rain-
565 fall and climate using Tropical Rainfall Measuring Mission (TRMM) satellite data and
566 limited rain gauge ground observations. *Journal of Applied Meteorology and Climatology*
567 54(3):541–555

568 NCL (2016) The NCAR Command Language (Version 6.3.0) [Software]. Boulder, Colorado:
569 UCAR/NCAR/CISL/TDD <http://dx.doi.org/10.5065/D6WD3XH5>

570 Negrón Juárez RI, Li W, Fu R, Fernandes K, de Oliveira Cardoso A (2009) Comparison of
571 precipitation datasets over the tropical South American and African continents. *Journal*
572 *of Hydrometeorology* 10(1):289–299

573 Nicholson S, Klotter D, Zhou L, Hua W (2019) Validation of satellite precipitation estimates
574 over the Congo Basin. *Journal of Hydrometeorology* 20(4):631–656

575 Nicholson SE (2018) The ITCZ and the seasonal cycle over equatorial Africa. *Bulletin of the*
576 *American Meteorological Society* 99(2):337–348

577 Nicholson SE, Some B, McCollum J, Nelkin E, Klotter D, Berte Y, Diallo BM, Gaye I,
578 Kpabeba G, Ndiaye O, Noukpozoukou JN, Tanu MM, Thiam A, Toure AA, , Traore AK
579 (2003) Validation of trmm and other rainfall estimates with a high-density gauge dataset

580 for West Africa. Part II: Validation of trmm rainfall products. *J Appl Meteor* 42:1355–1368

581 Penlap K, Matulla C, Storch H, Mkankam F kanga (2004) Downscaling of GCM scenarios to
582 assess precipitation changes in the little rainy season (March-June) in Cameroon. *Climate*
583 *Research* 26:85–96

584 Poccard I, Janicot S, Camberlin P (2000) Comparison of rainfall structures between
585 NCEP/NCAR reanalyses and observed data over tropical Africa. *Clim Dyn* 16:897–915

586 Pohl B (2007) L'oscillation de Madden-Julian et la variabilité pluviométrique régionale en
587 Afrique subsaharienne. Ph D thesis, Université de Bourgogne

588 Pokam WM, Djotang LAT, Mkankam FK (2012) Atmospheric water vapor transport and
589 recycling in Equatorial Central Africa through NCEP/NCAR reanalysis data. *Climate*
590 *Dynamics* 38(9-10):1715–1729

591 Raghavendra A, Zhou L, Jiang Y, Hua W (2018) Increasing extent and intensity of thunder-
592 storms observed over the Congo Basin from 1982 to 2016. *Atmospheric Research* 213:17–26

593 Raghavendra A, Zhou L, Roundy PE, Jiang Y, Milrad SM, Hua W, Xia G (2020) The MJO's
594 impact on rainfall trends over the Congo rainforest. *Climate Dynamics* pp 1–13

595 Roads J, Chen SC, Kao J, Langley D, Glatzmater G (1992) Global aspects of the los alamos
596 general circulation model hydrologic cycle. *Journal of Geophysical Research: Atmospheres*
597 97(D9):10,051–10,068

598 Roudier P, Ducharne A, Feyen L (2014) Climate change impacts on runoff in West Africa: a
599 review. *Hydrology and Earth System Sciences* 18(7):2789–2801

600 Samba G, Nganga D (2012) Rainfall variability in Congo-Brazzaville: 1932–2007. *Interna-*
601 *tional Journal of Climatology* 32(6):854–873

602 Sandjon AT, Nzeukou A, Tchawoua C (2012) Intraseasonal atmospheric variability and its
603 interannual modulation in Central Africa. *Meteorology and Atmospheric Physics* 117(3-
604 4):167–179

605 Sandjon AT, Nzeukou A, Tchawoua C, Sonfack B, Siddi T (2014) Comparing the patterns
606 of 20–70 days intraseasonal oscillations over Central Africa during the last three decades.
607 *Theoretical and applied climatology* 118(1-2):319–329

608 Sassen K, Krueger SK (1993) Toward an empirical definition of virga: Comments on ÅIJs

609 virga rain that evaporates before reaching the ground?â. Monthly weather review
610 121(8):2426–2428

611 Scheel M, Rohrer M, Huggel C, Santos D Villar, Silvestre E, Huffman G (2011) Evaluation of
612 TRMM multi-satellite precipitation analysis (TMPA) performance in the Central Andes
613 region and its dependency on spatial and temporal resolution. Hydrol Earth Syst Sci
614 15:2649–2663. doi:10.5194/hess-15-2649-2011

615 Sultan B, Janicot S (2003) The West African monsoon dynamics. Part II: The âpreon-
616 setâ and âJonsetâ of the summer monsoon. Journal of climate 16(21):3407–3427

617 Sultan B, Janicot S (2004) La variabilit  climatique en Afrique de l’Ouest aux  chelles saison-
618 ni res et intra-saisonnieres I: mise en place de la mousson et variabilit  intra-saisonnier
619 de la convection. S cheresse 15(4):1–10

620 Sun K, Zhu L, Cady-Pereira K, Chan Miller C, Chance K, Clarisse L, Coheur PF,
621 Gonz lez Abad G, Huang G, Liu X, et al (2018) A physics-based approach to oversample
622 multi-satellite, multispecies observations to a common grid. Atmospheric Measurement
623 Techniques 11(12)

624 Suzuki T (2011) Seasonal variation of the ITCZ and its characteristics over central Africa.
625 Theoretical and Applied Climatology 103(1-2):39–60

626 Tamoffo AT, Moufouma-Okia W, Dosio A, James R, Pokam WM, Vondou DA, Fotso-Nguemo
627 TC, Guenang GM, Kamsu-Tamo PH, Nikulin G, et al (2019a) Process-oriented assessment
628 of RCA4 regional climate model projections over the Congo Basin under [Formula: see text]
629 and [Formula: see text] global warming levels: influence of regional moisture fluxes. Climate
630 dynamics

631 Tamoffo AT, Vondou DA, Pokam WM, Haensler A, Yepdo ZD, Fotso-Nguemo TC, Tchotchou
632 LAD, Nouayou R (2019b) Daily characteristics of Central African rainfall in the REMO
633 model. Theoretical and Applied Climatology 137(3-4):2351–2368

634 Tanessong RS, Igri PM, Vondou DA, Tamo PK, Kamga FM (2014) Evaluation of probabilistic
635 precipitation forecast determined from WRF forecasted amounts. Theoretical and applied
636 climatology 116(3-4):649–659

637 Tanessong RS, Vondou DA, Djomou ZY, Igri PM (2017) WRF high resolution simulation of

638 an extreme rainfall event over Douala (Cameroon): A case study. *Modeling Earth Systems*
639 and *Environment* 3(3):927–942

640 Taylor CM, Fink AH, Klein C, Parker DJ, Guichard F, Harris PP, Knapp KR (2018) Earlier
641 seasonal onset of intense mesoscale convective systems in the Congo Basin since 1999.
642 *Geophysical Research Letters* 45(24):13–458

643 Tchotchou LA Djotang, Mkankam-Kamga F (2010) Sensitivity of the simulated African
644 monsoon of summers 1993 and 1999 to convective parameterization schemes in RegCM3.
645 *Theor Appl Climatol* 100:207–220

646 Tom M, Maarten A van, Paula V Silva (2010) Assessing progress on integrating disaster
647 risk reduction and climate change adaptation in development processes. *Strengthening*
648 *Climate Resilience Discussion Paper 2*

649 Vondou AD, Nzeukou A, Lenou A, Mkankam K (2010a) Seasonal variations in the diur-
650 nal patterns of convection in cameroon–nigeria and their neighboring areas. *Atmospheric*
651 *Science Letters* 11:290–300

652 Vondou AD, Nzeukou A, Mkankam K (2010b) Diurnal cycle of convective activity over the
653 West of Central Africa based on meteosat images. *International Journal of Applied Earth*
654 *Observation and Geoinformation* 12:S58–S62

655 Vrieling A, De J Leeuw, Said Y M (2013) Length of growing period over africa: Variability
656 and trends from 30 years of NDVI time series. *Remote Sensing* 5(2):982–1000

657 Washington R, James R, Pearce H, Pokam WM, Moufouma-Okia W (2013) Congo Basin
658 rainfall climatology: can we believe the climate models? *Philosophical Transactions of the*
659 *Royal Society B: Biological Sciences* 368(1625):20120,296

660 Wilks S D, Dmowska R, Harmatan D, Rossby T H (2006) *Statistical methods in the at-*
661 *mospheric sciences*. Second edition, Elseiver, International Geophysics Sciences, Academic
662 Press

663 Yepdo Z Djoumou, Monkam D, Lénouo A (2009) Spatial variability of rainfall regions in
664 West Africa during the 20th century. *Atmos Sci Let* 10:9–13

665 Yin X, Gruber A, Arkin P (2004) Comparison of the GPCP and CMAP merged gauge–
666 satellite monthly precipitation products for the period 1979–2001. *Journal of Hydromete-*

667 orology 5(6):1207–1222

668 Zebaze S, Lenouo A, Tchawoua C, Gaye AT, Kamga FM (2017) Interaction between moisture
669 transport and Kelvin waves events over Equatorial Africa through ERA-interim. Atmo-
670 spheric Science Letters 18(7):300–306

671 Zhou L, Tian Y, Myneni RB, Ciais P, Saatchi S, Liu YY, Piao S, Chen H, Vermote EF,
672 Song C, et al (2014) Widespread decline of Congo rainforest greenness in the past decade.
673 Nature 509(7498):86–90

674 **List of Tables**

675 1 Summary of available in situ rainfall observations in Cameroon from 1998 to present. N.A sta

676 2 Contingency table 32

677 **List of Figures**

678 1 Study domain with the five agro-ecological zones in Cameroon. The ombro thermic diagrams

679 2 (A) Study domain (Cameroon) with the Congo Basin (solid red line). (B) Geographical repart

680 3 Mean monthly accumulated (mm) rainfall for different stations. Stations are representative of

681 4 Mean annual correlation for the mentioned stations. 36

682 5 Mean annual biases (mm/year) over the available data period for different stations 37

683 6 Mean monthly tropical rain belt position over Cameroon for the period 1990 to 2015 between

684 7 Daily time series of accumulated rainfall over Maroua, Garoua and Ngaoundere for the years

685 8 Daily time series of accumulated rainfall over Bertoua, Douala and Ebolowa for the years 199

686 9 Categorical indices for daily rainfall and linear regression fitting (scatter plots) for years 1998

687 10 Sensitivity of categorical indices (a: BIAS (frequency bias), b: ETS, c: POD and d: POFD) w

688 11 Interannual Hovmöller diagrams of the monthly accumulated convective rainfall and climatolo

689 12 Spatiotemporal distribution of the 90th percentile of the monthly accumulated convective rain

690 13 Same as Fig. 12, but for 3B43. 45

691 14 Correlation, mean absolute error (MAE), root mean square error (RMSE) and the mean bias

Table 1

Summary of available in situ rainfall observations in Cameroon from 1998 to present. N.A stands for Not Available.

Station Name	Temporal Record	Lat [°N]	Lon [°E]	Station Elevation [m]
Abong-Mbang	1998-2008	3.96	13.18	693
Akonolinga	1998-2008	3.8	12.25	671
Ambam	1998-2008	2.38	11.26	602
Bafia	1998-2008	4.73	11.23	501
Bamenda	1998-2008	5.93	10.15	1668
Banyo	1998-2008	6.73	11.8	1110
Bertoua	1998-2008	4.58	13.68	668
Douala	1998-2008	4.01	9.73	5
Dschang	1998-2008	5.45	10.06	1339
Ebolowa	1998-2008	2.91	11.15	603
Garoua	1998-2008	9.33	13.38	242
Kaele	1998-2005	10.08	14.43	388
Koundja	1998-2005	5.63	10.73	1217
Kongsamba	1998-2008	4.95	9.93	816
Maroua-Salak	1998-2000	10.27	14.13	422
Newsonne	1998-2003/2005-07	4.06	9.36	N.A
Ngaoundere	1998-2005	7.35	13.25	1130
Mpundu	1998-2007	4.23	9.40	N.A
Mukunje	1998-2007	4.58	9.50	N.A
Touboro	1998-2005	7.76	15.36	500
Yaounde	1998-2000	3.51	11.28	760

Table 2

Contingency table

		Observed Rain	
		Yes	No
Estimated Rain	Yes	h	f
	No	m	c

Agro-Ecological Zones Map of Cameroon

Sudano-Sahelian zone (100 353 km²)

Rainfall: 400 to 1200 mm/year
soil type: great diversity: ferruginous, leached, hydromorphs, alluvial deposits, lithosols, vertisols, etc.
cultures: cotton, millet, sorghum, cowpea, onion, sesame seeds

Highs savannahs Zone (123 077 km²)

Rainfall: 1500 mm/year, 150 rainy days
soil type: permeable, medium water holding capacity, brown or red ferrallitic soils and hydromorphic soils
cultures: corn, cotton, millet, sorghum, yam, potato

Highlands Zone (31 192 km²)

Rainfall: 1500 to 2000 mm/year, 180 rainy days
soil type: Very fertile and suitable for agricultural activities, young on steep slopes, leached in the old plateaus, B horizon of illuviation in closed depressions, plateaus enriched with volcanic materials.
cultures: cocoa, coffee, corn, dry beans, potatoes, etc

Uni-modal forest Zone (45 658 km²)

Rainfall: 2500 to 4000 mm/year, single mode diet
soil type: Volcanic slopes, sediments of rocky origin along the coast
cultures: cocoa, banana, coffee, plantain, palm oil, ginger, pepper

Bi-modal forest Zone (165 770 km²)

Rainfall: 1500 to 2000 mm/year, two distinct wet seasons
soil type: ferrallitic, acidic, clayey, low nutrient retention capacity
cultures: cocoa, coffee, cassava, plantain, corn, palm oil, pineapple

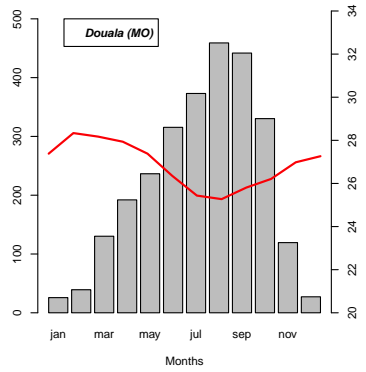
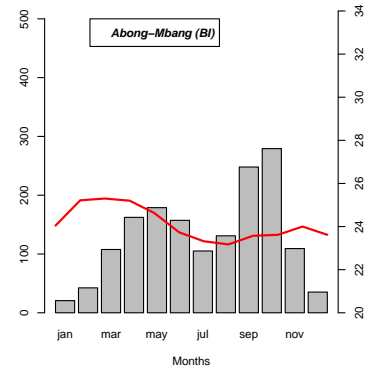
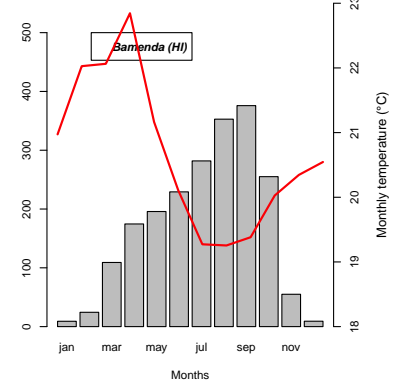
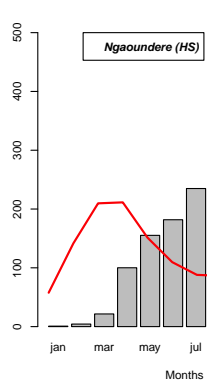
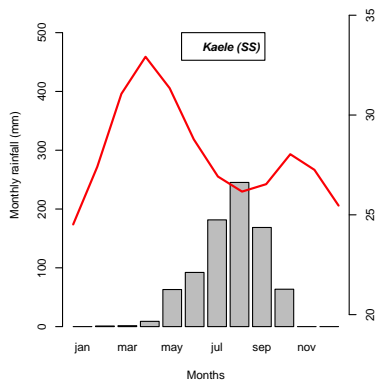
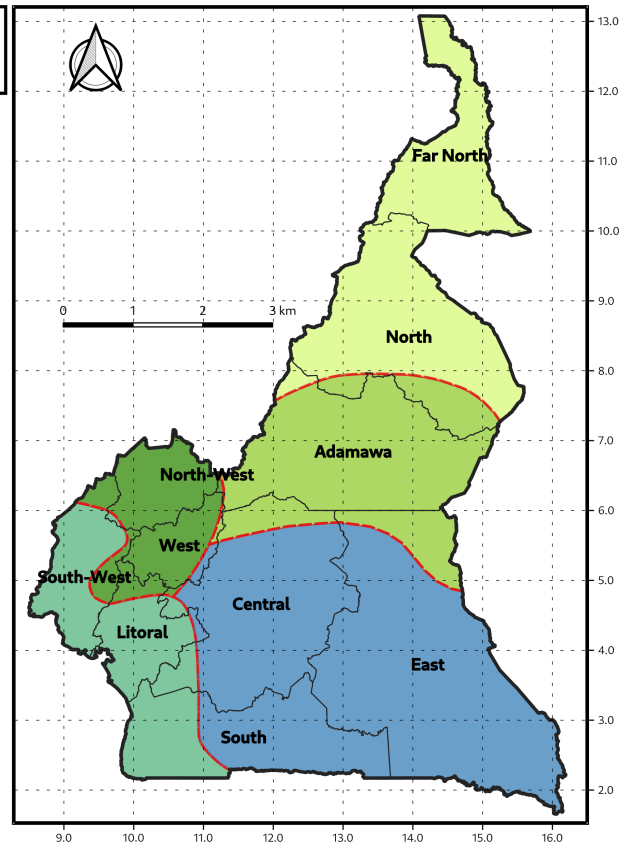


Fig. 1. Study domain with the five agro-ecological zones in Cameroon. The ombrothermic diagrams are also represented for five stations, each station representing an agroecological zone.

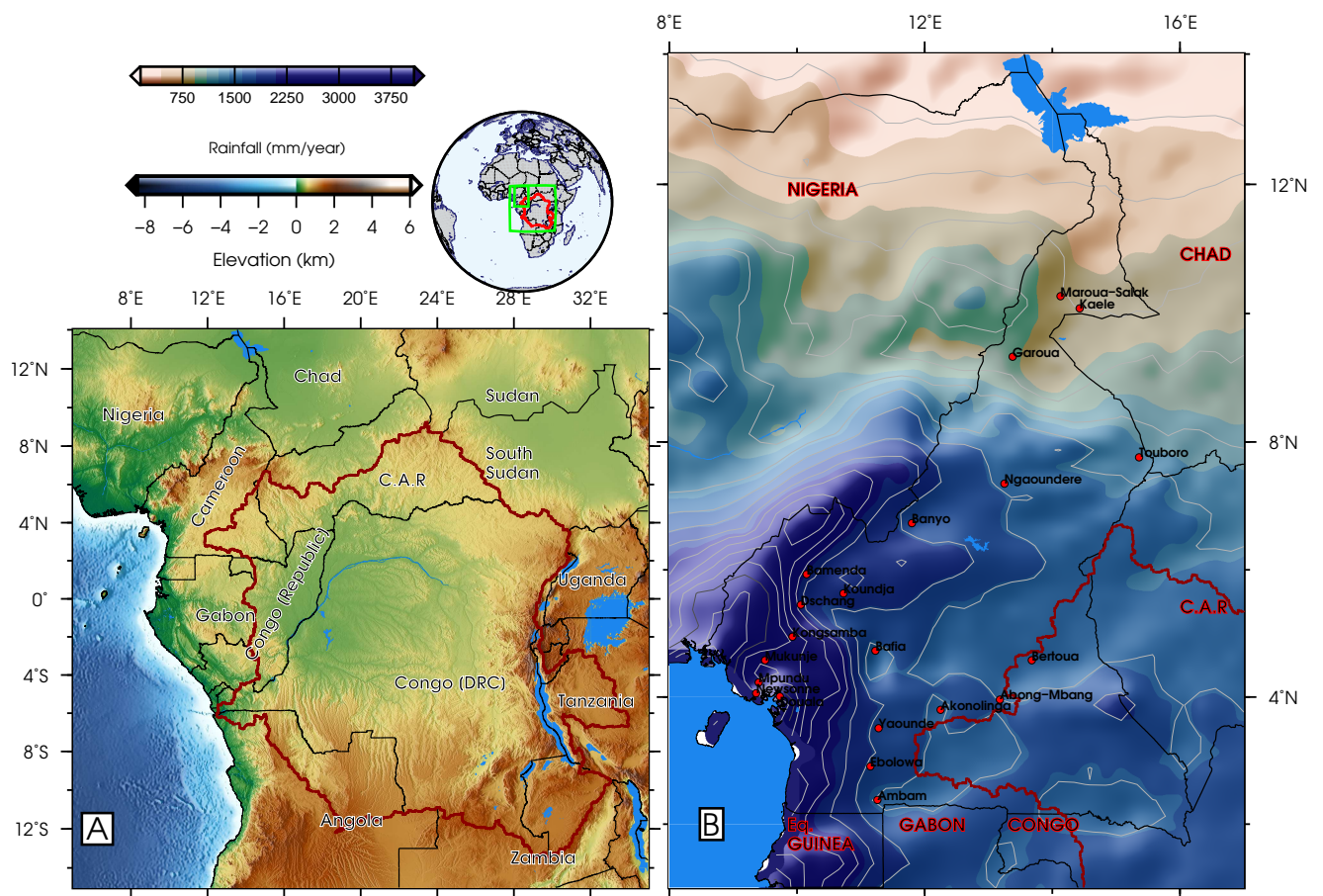


Fig. 2. (A) Study domain (Cameroon) with the Congo Basin (solid red line). (B) Geographical repartition of synoptic weather stations in Cameroon including the climatology of annual accumulated rainfall from CHIRPS data (1983-2013).

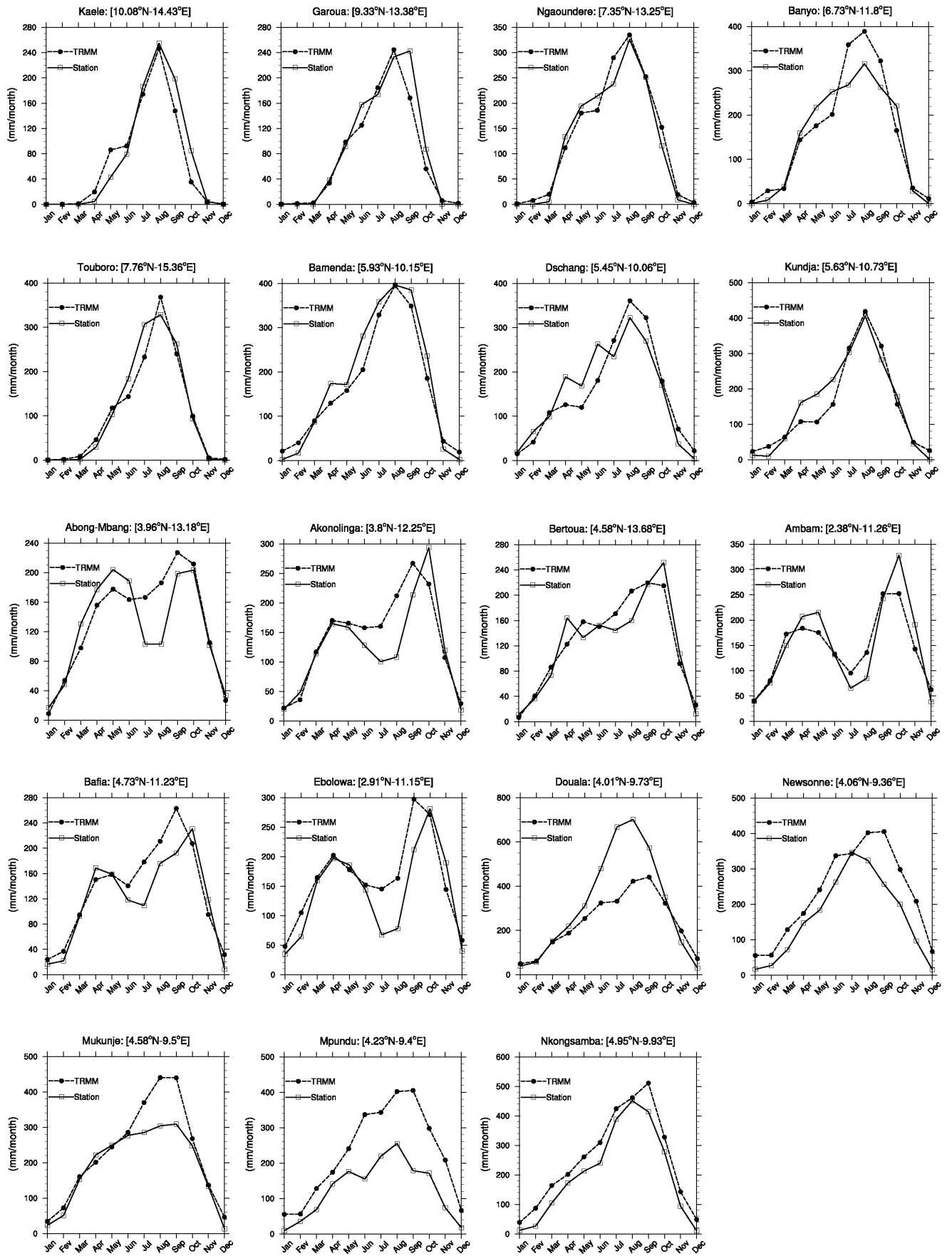


Fig. 3. Mean monthly accumulated (mm) rainfall for different stations. Stations are representative of the different agro-ecological zones as presented in Figure 2.

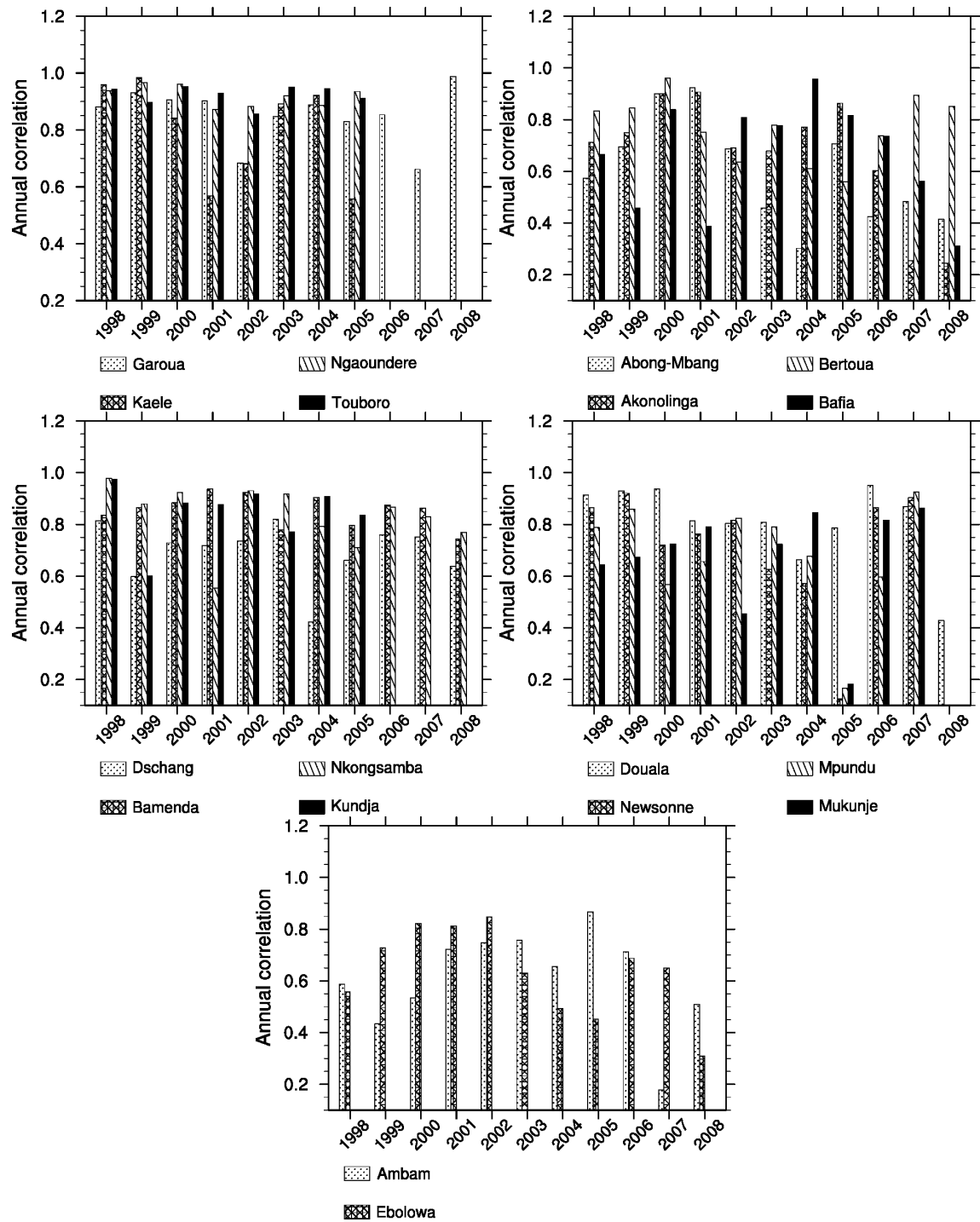


Fig. 4. Mean annual correlation for the mentioned stations.

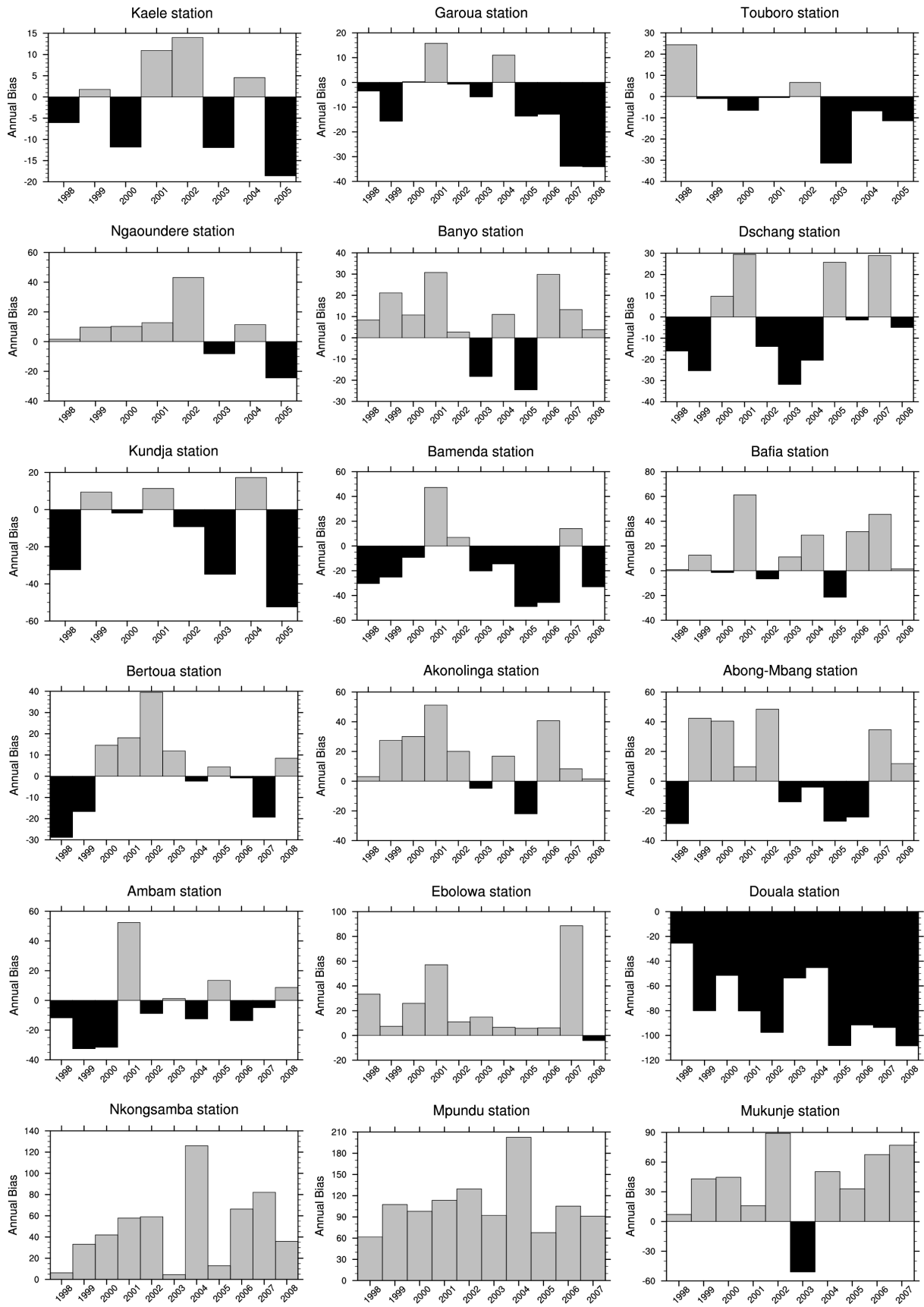


Fig. 5. Mean annual biases (mm/year) over the available data period for different stations

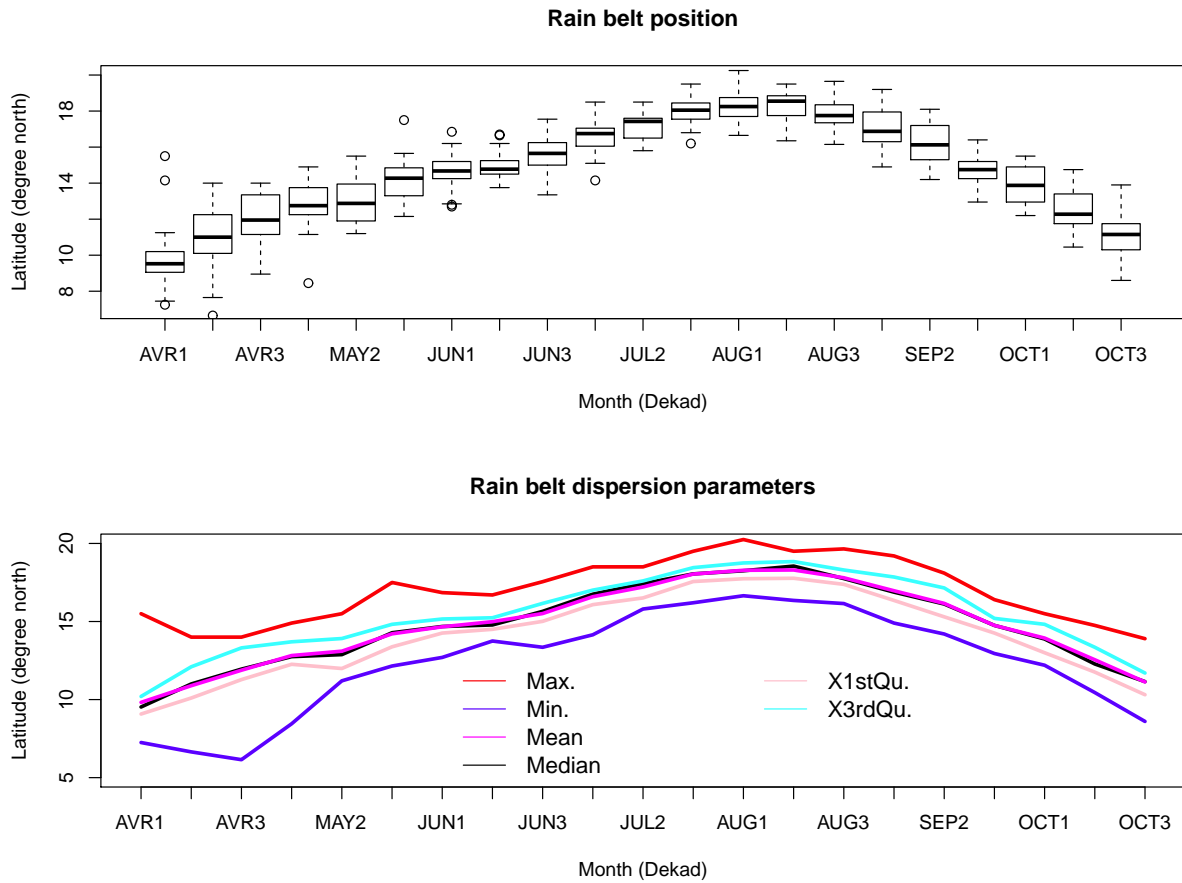


Fig. 6. Mean monthly tropical rain belt position over Cameroon for the period 1990 to 2015 between april and october (from november to early march, the tropical rain belt is localized around 5°N, its southernmost position).

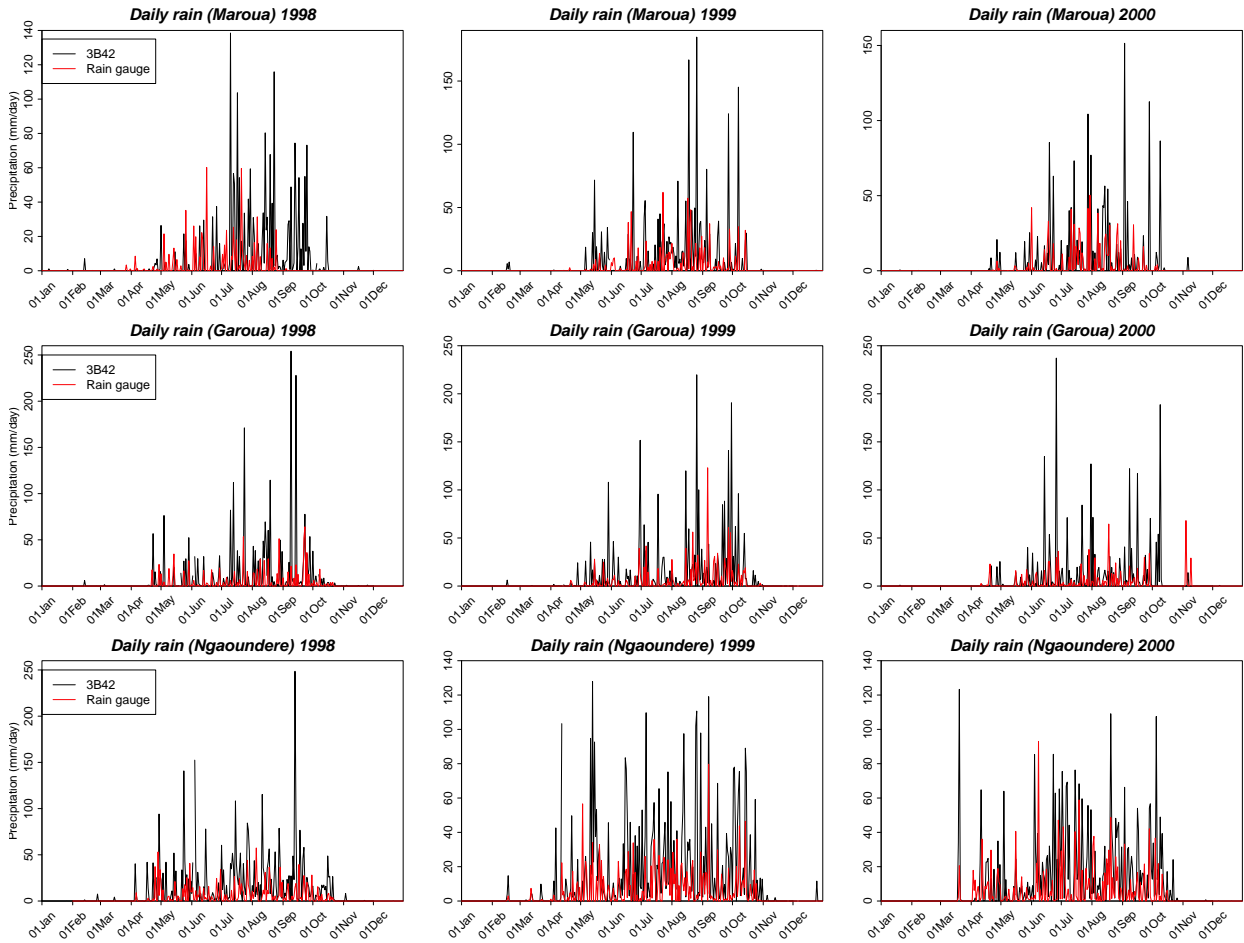


Fig. 7. Daily time series of accumulated rainfall over Maroua, Garoua and Ngaoundere for the years 1998, 1999 and 2000.

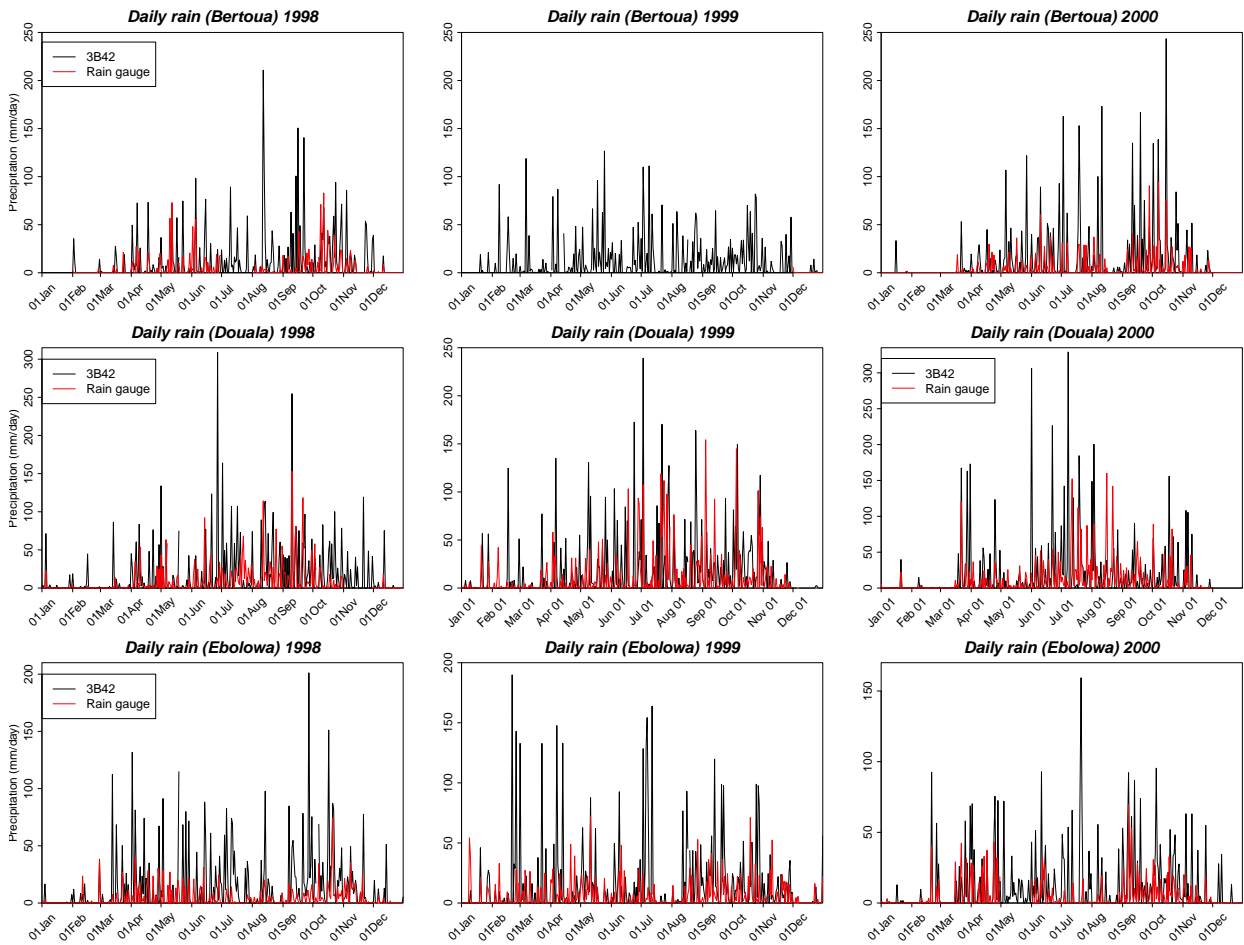


Fig. 8. Daily time series of accumulated rainfall over Bertoua, Douala and Ebolowa for the years 1998, 1999 and 2000.

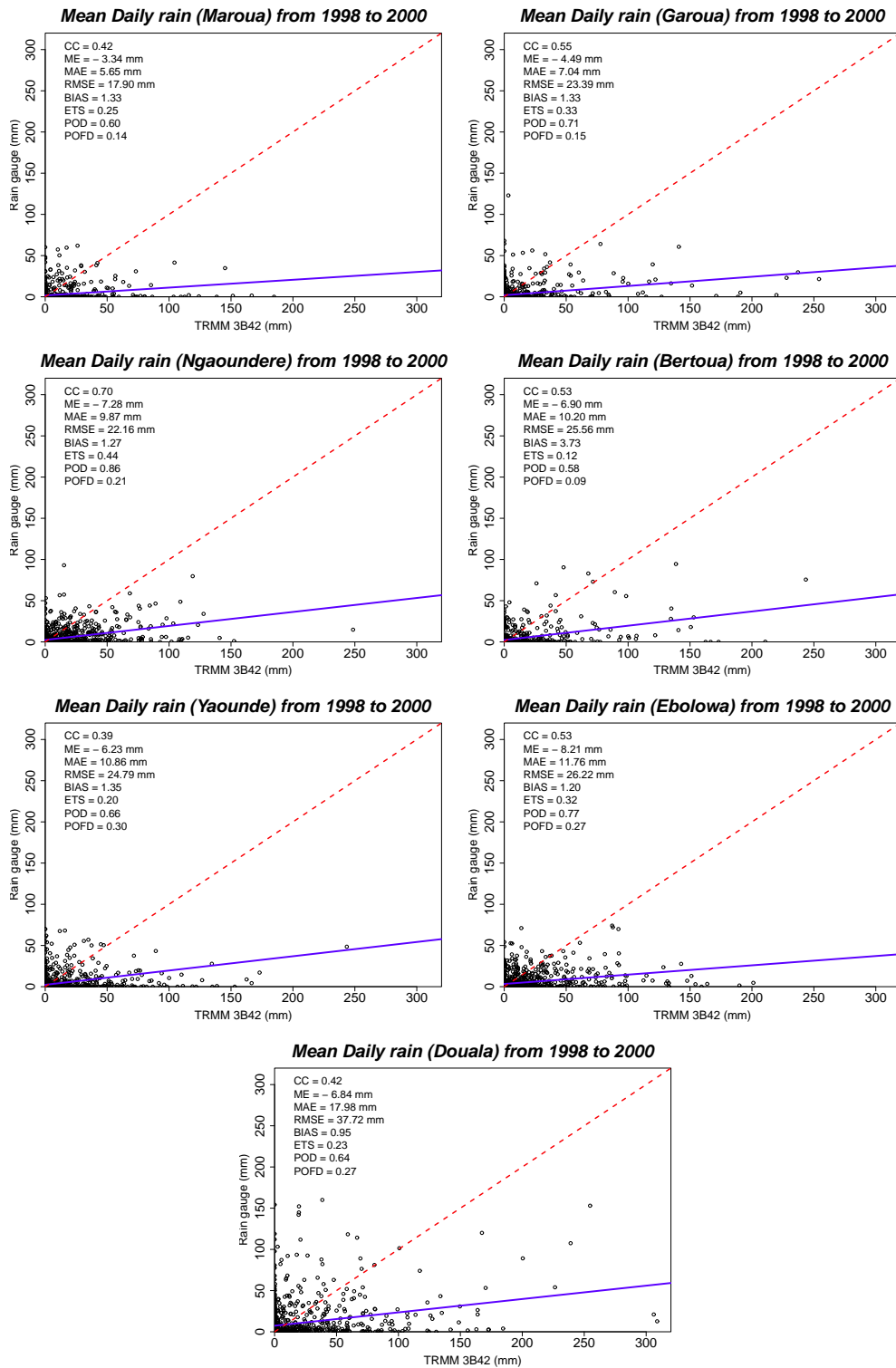


Fig. 9. Categorical indices for daily rainfall and linear regression fitting (scatter plots) for years 1998 to 2000 for different stations. Plots are shown with a threshold of 1mm/day

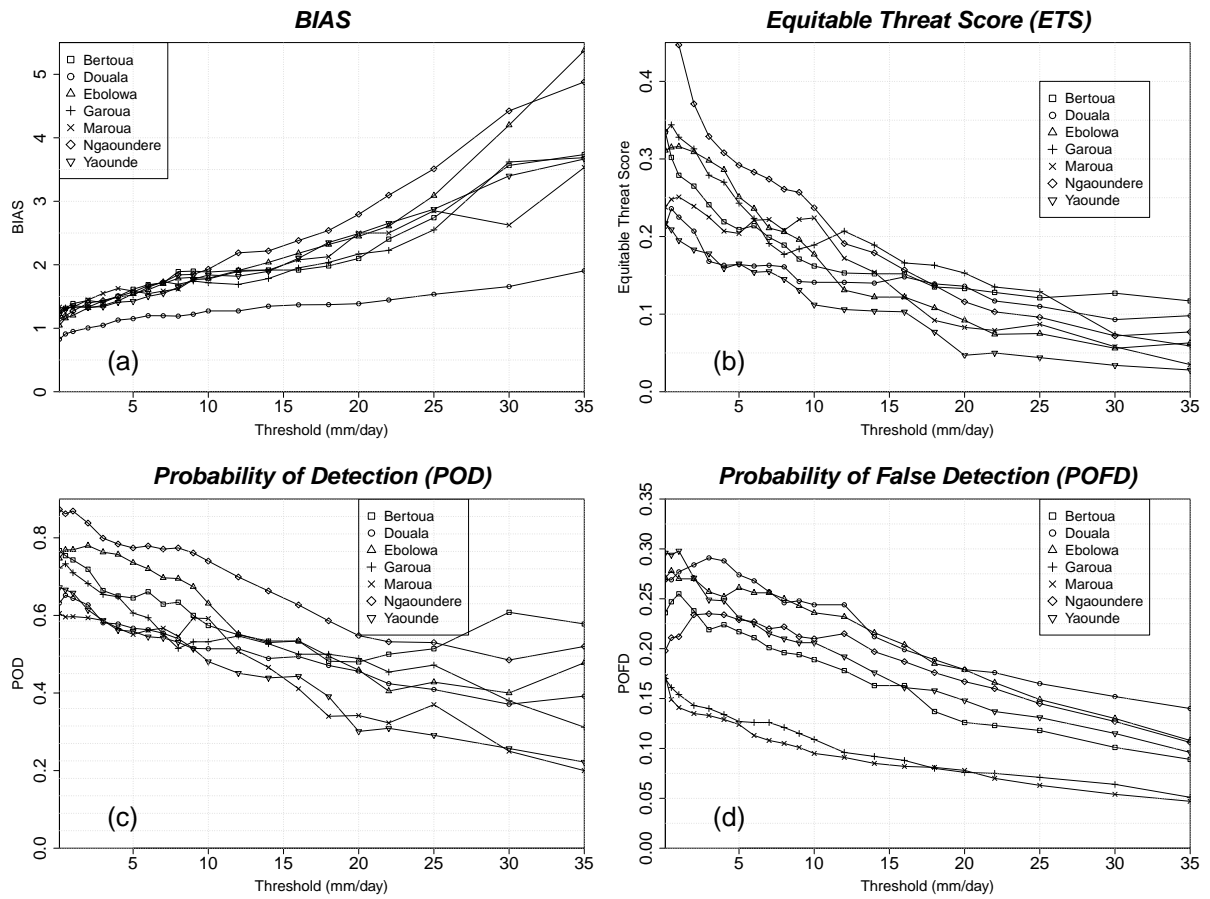


Fig. 10. Sensitivity of categorical indices (a: BIAS (frequency bias), b: ETS, c: POD and d: POFD) with different daily precipitation thresholds. Indices are computed for the available stations for the period 1998 to 2000 according to the contingency table presented in Table 2.

TRMM 3A12 (1998-2008), Average [8E-17E] (mm/month)

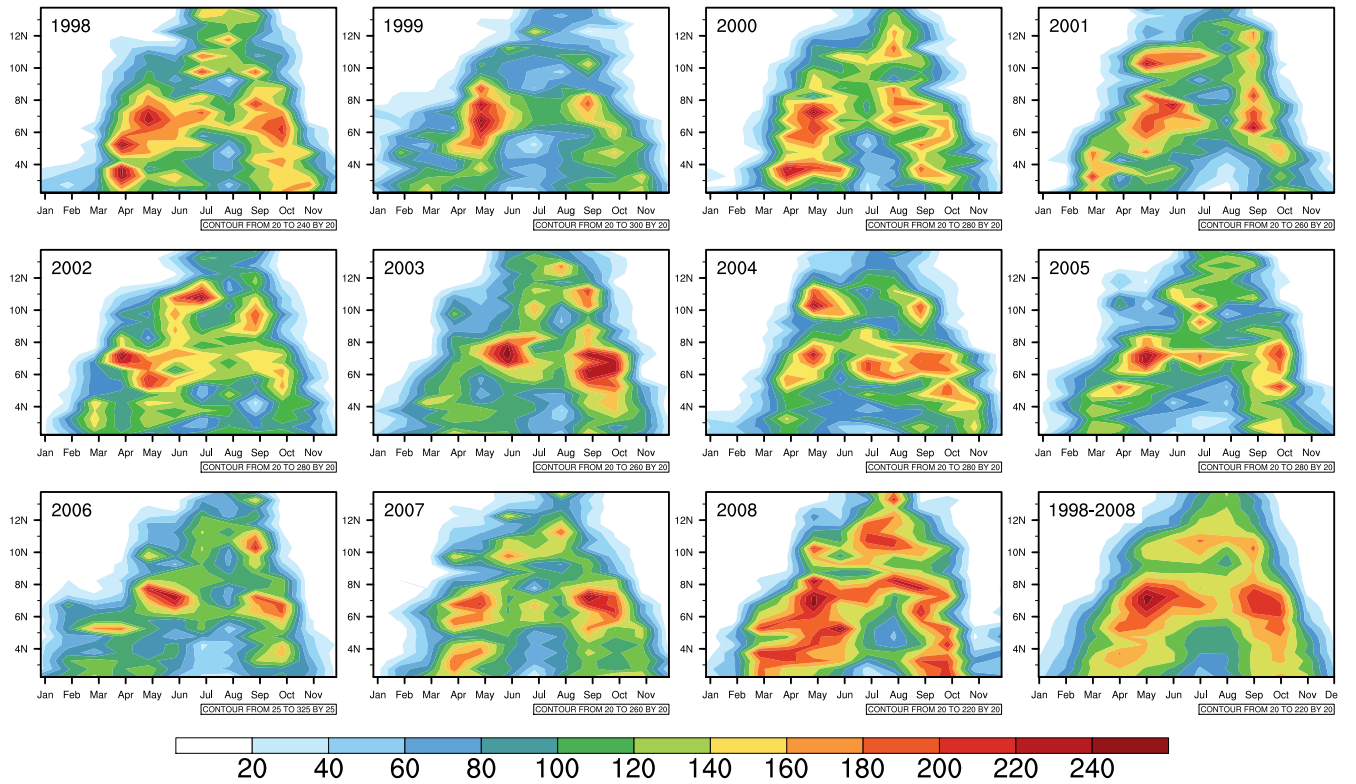


Fig. 11. Interannual Hovmöller diagrams of the monthly accumulated convective rainfall and climatology (1998-2008) from TRMM 3B12 products averaged over 8°E–17°E.

(1)-Convective(3A12) and (2)-non-Convective(3B42-3A12) Rainfall
90 Percentiles (mm/month)

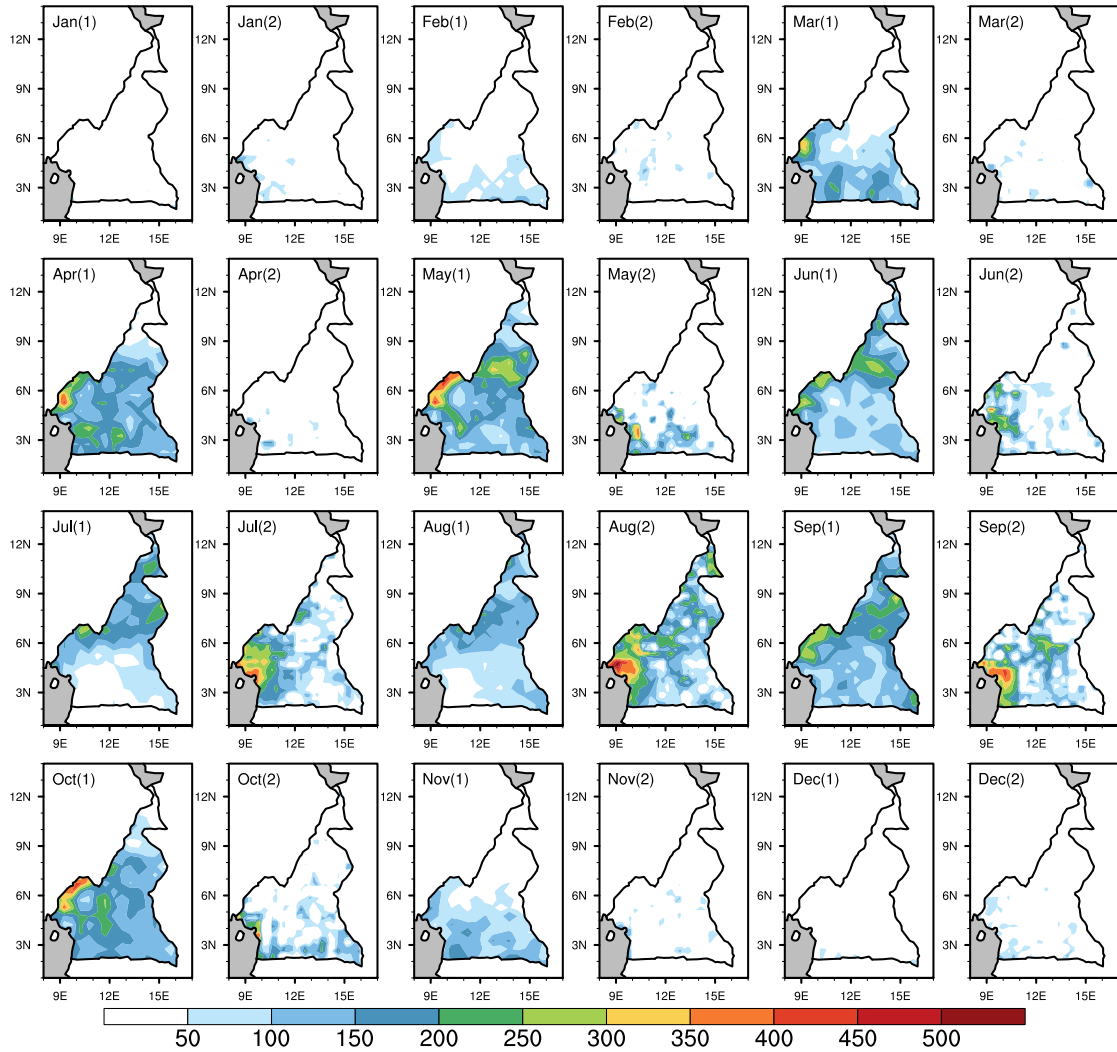


Fig. 12. Spatiotemporal distribution of the 90th percentile of the monthly accumulated convective rainfall climatology (3A12) and monthly accumulated non-convective rainfall climatology (3B42 - 3A12). The climatology is computed from 1998–2008. (1) refers to convective rainfall and (2) refers to non-convective rainfall or large scale rainfall (difference between 3B42 and 3A12).

(1)-Convective(3A12) and (2)-non-Convective(3B43-3A12) Rainfall
90 Percentiles (mm/month)

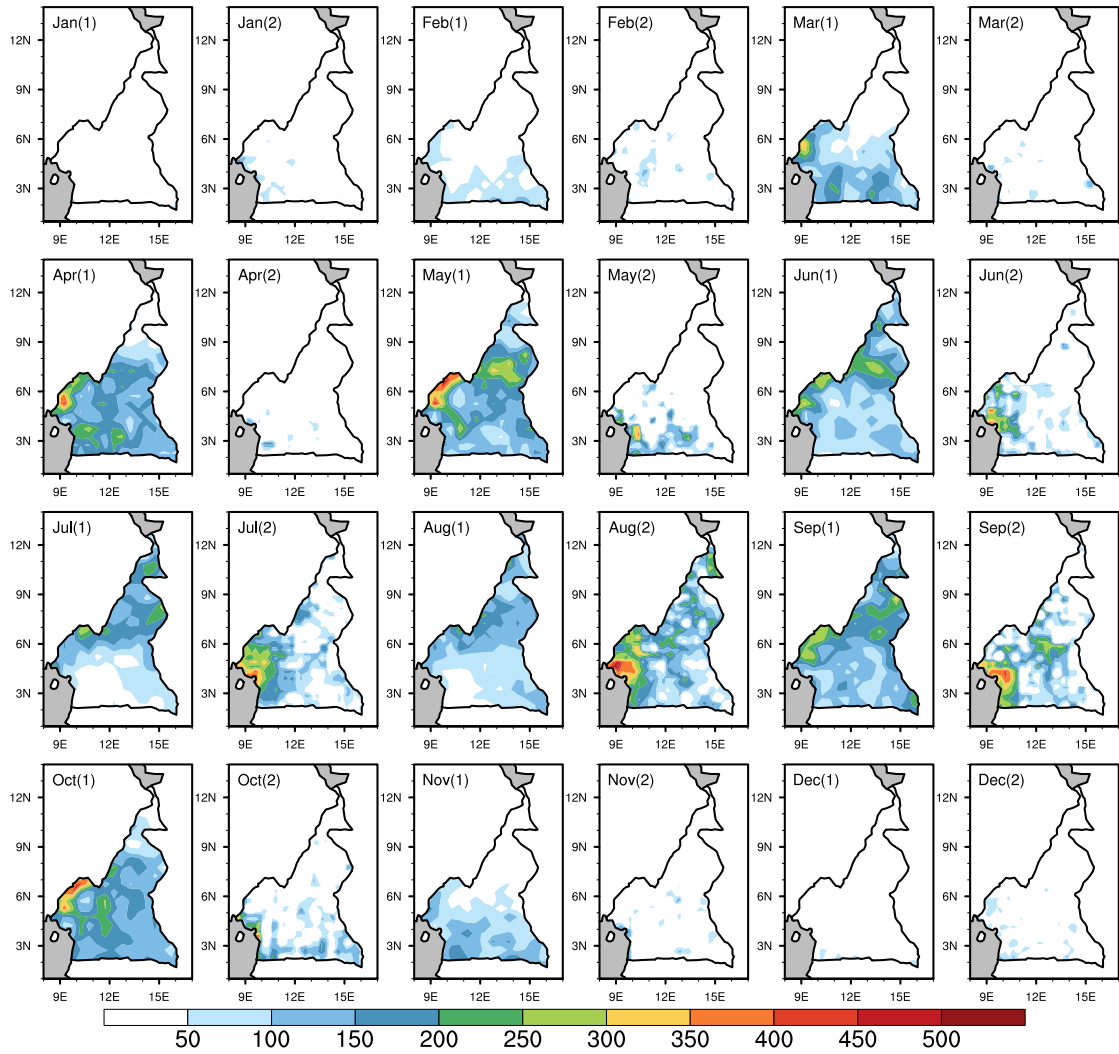


Fig. 13. Same as Fig. 12, but for 3B43.

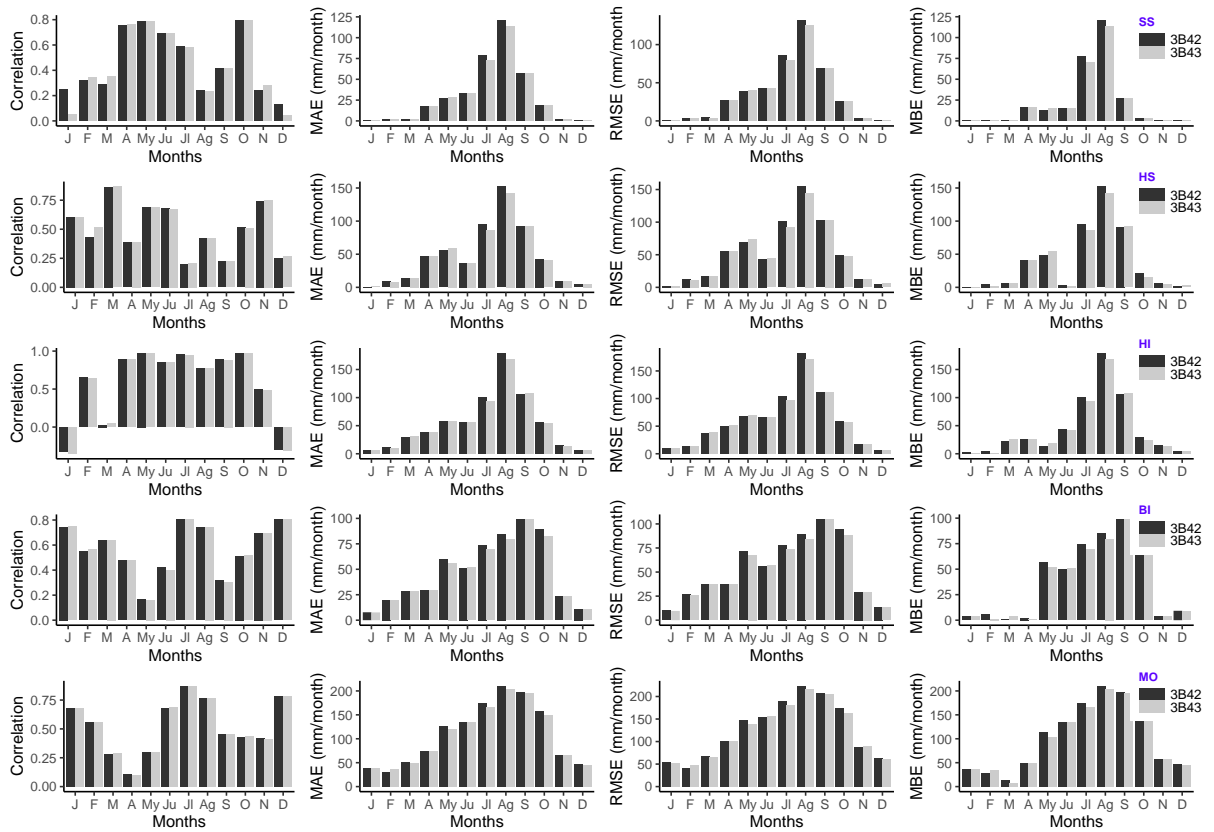


Fig. 14. Correlation, mean absolute error (MAE), root mean square error (RMSE) and the mean bias between the mean monthly accumulated convective rainfall (3A12) and mean monthly accumulated total rainfall from 3B42 and 3B43. SS : Sudano-sahelian zone, HS : Highers Savannahs zone, HI : Highlands zone, BI : Bi-modal forests zone, MO : Mono-modal forests zone